Design and Analysis of Solar Water Pumping for Drip Irrigation in Iran

by

© Mohammad Zamanlou

A Thesis submitted to the School of Graduate Studies in partial fulfillment of the requirements for the degree of

Master of Engineering
Faculty of Engineering & Applied Science

MEMORIAL UNIVERSITY

February 2021

ST. JOHN'S NEWFOUNDLAND & LABRADOR CANADA

Abstract

In this thesis, a solar water pumping system is designed and studied for drip irrigation of a 14.7 hectare grape garden in Iran. Firstly, two kinds of solar-powered water pump systems were designed and studied. The difference between the systems is the storage type. One system uses a battery bank, and the other is with a water tank storage. The first system is designed using Lorentz compass3 software and includes a 6-inch 18.5 KW submersible pump. HOMER Pro software was used to model the second system and resulted in a 6-inch 11 KW submersible pump, and 44.4kw PV modules rated capacity and 144 KWh Battery Bank size. This research indicates using a storage system allows constant water flow for irrigation in solar water pumping and comparing the results, the research shows that using a battery bank is more economical than a water tank storage system.

Secondly, a cost-effective IoT-based SCADA system for a solar water pumping system was developed. The IoT-based SCADA is comprised of a raspberry pi zero W, Arduino nano, camera, SIM 5320A 3G module, voltage, current, and light sensors. We used Node-RED to design a graphical user interface and published it securely to the worldwide internet. This allows a user to connect to the server via an IP address and monitor and control the system. The implementation of the project resulted in an open-source server and cost around CAD$ 162.38.

Acknowledgements

Thanks to my supervisor Dr. Tariq M. Iqbal for his continues support and my course instructors Dr. Siu O'Young and Dr. Anand Sharan for the knowledge they shared with me. Thanks to Avrin Goom Azaran company for funding my degree and sponsorship and project supports and funds from the Memorial University, Faculty of Engineering & Applied Science. My sincerest thanks to my mother, my father and my uncle for their support and prayers. Finaly, thanks to all my friends who supported me and enlightend the Master of Engineering path for me.

Table of Contents

Lists of Tables

List of Figures

Chapter 1 Introduction

1.1 Background

Iran is a developing country where most of the electricity is generated from its limited fossil fuel resources. These resources are polluting the environment and causing global warming, and they are also limited. Figure 1.1 shows the graph for electricity generation from different types of sources in Iran. Due to the ongoing increase in demand for electrical energy, technologies that use clean resources need to be studied, implemented, improved to support the demand and help protect our environment. Therefore, renewable energies, especially solar energy, have become the main interest of researchers worldwide, especially in Iran. Nowadays, many applications of solar photovoltaic systems are being studied. One important application of solar PV systems is in agriculture and for irrigation. It is essential to expand these systems in agriculture because it plays a vital role in the development of Iran.[1]–[4]

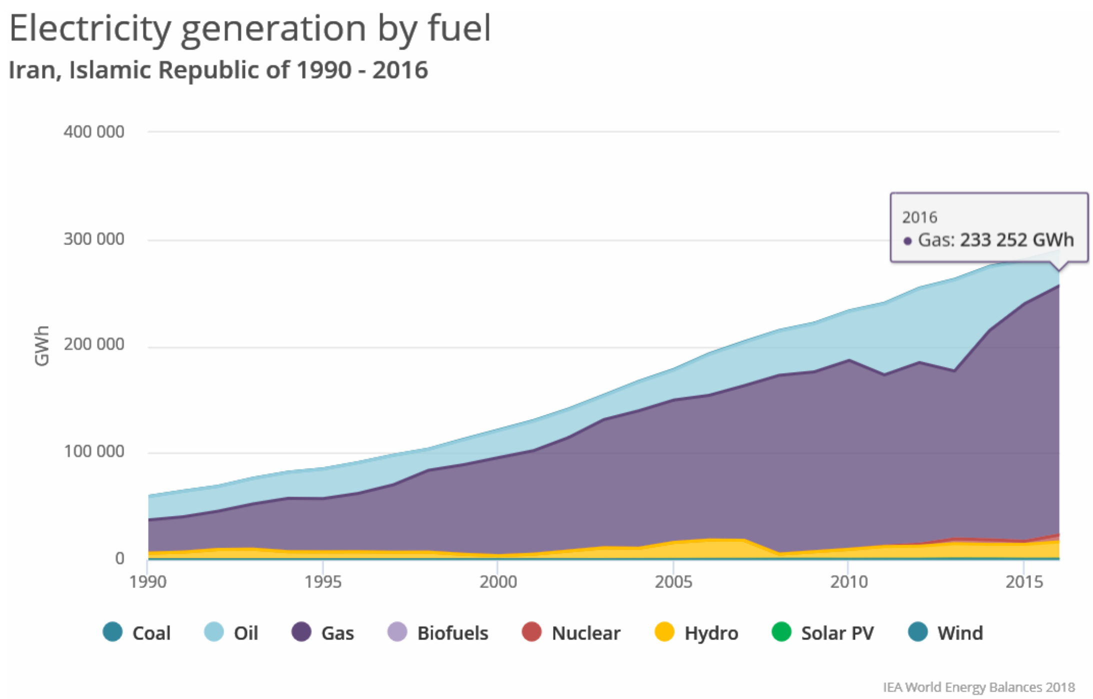

Figure 1.1: Graph for electricity generation in Iran from different sources over 26 years (Image from IEA)

As shown in Figure 1.2, there is a huge water crisis due to mis-use of water in irrigation in Iran. Among all types of irrigation systems, micro-irrigation is the most efficient way of irrigating crops. In [5], the study shows that micro-irrigation has 60% less water waste comparing to the flood irrigation method. In this method, water is directly supplied into the roots of the crops, which results in very little loss of water and higher crop yields. In this irrigation type, a water pump supplies water with pressure into the pipes and drippers. That being said, it is crucial to develop such a system in that area because there is an extreme environmental crisis is happening in Iran due to the misuse of water in irrigation, which is mainly using traditional methods such as flood irrigation. Figure 1.3 shows the general schematic diagram of a solar water pumping system with all the components that are implementable in it.[6], [7]

Figure 1.2: The condition of Urmia Lake over the course of 15 years (image from Google)

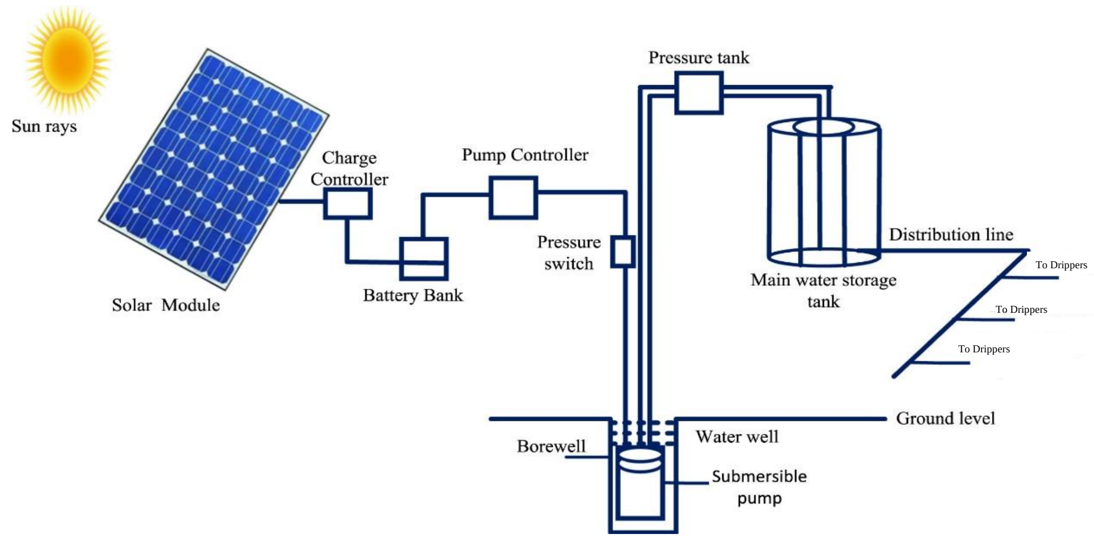

Figure 1.3: Schematic diagram of a solar water pumping system

In this research, solar energy is used to power the pumping system. First, a complete water requirement analysis of the garden was done using the Food and Agriculture Organization (FAO) tools. Based on the results of the water analysis which presents the load size of the project, three types of solar water pumping systems were designed and analyzed using Lorentz Compass 3 and HOMER Pro software; it includes one system without any storage, another with a battery bank, and last one with a water tank storage.

The case study in this project was a 14.74-hectare grape garden in Urmia, West Azerbaijan, Iran (37° 26’17.7” N 45° 08’33.7” E), which is shown in Figure 1.4.

Figure 1.4: A photograph of the site from google maps

1.2 Problem statement

The goal of this research is to design a solar water pumping system for irrigation of a 14.7 ha grape garden and design a low cost IoT-based SCADA for monitoring and controlling.

1.2.1 Technical difficulties

First, the number of researches who worked on this topic is very limited in Iran which makes it difficult to find data and use raw resources to complete the project.

Second, the load is an agricultural crop, grapes in this case, and the supply is an electrical entity. Therefore, the analysis and sizing of the load requires finding and using combination of traditional methods and technical scientific methods.

Last, the selected site is a place in Iran and the study is done in Canada in which case there are a lot of major differences between the places such as the type of the internet connection for developing a communication system. Therefore, it requires precise simulations and assumptions to implement the project which can also be implementable in Iran.

1.3 Expected contribtions

It aims, firstly, to organize a complete water requirement analysis for the grape garden which makes it possible to execute the load sizing.

Secondly, designing solar water pumping systems that can supply to load. In this goal, a comparison of using two types of storage systems is considered to be done, such as a battery storage system and a water tank.

Third, a MATLAB/Simulink dynamic and control model will be developed to study the response of the solar water pumping system with battery storage.

Finally, a low-cost IoT-based SCADA system will be developed to remotely monitor and control the solar pumping system in the field.

1.4 Thesis organization

Chapter 1 is the introduction of the thesis and involves a background around the topic and importance of selecting the topic, a problem statement and technical difficulties of the problem, and the expected contributions that will be made throughout the thesis.

Chapter 2 is the literature review of the thesis and presents the works that has been made until the date of the thesis.

Chapter 3 is the sizing and modelling of the project. In this chapter, a complete water requirement analysis of the grape garden was done using scientific tools and then three types of solar water pumping systems (without storage, with a battery storage system, and with a water tank) are designed and optimized.

Chapter 4 presents the dynamic modelling of a solar water pumping with battery storage system in MATLAB/Simulink and several controlling is implemented over the dynamic model. The model simulates the behavior of the solar water pumping system under different solar irradiance conditions.

Chapter 5 presents a communication system that was implemented to remotely monitor and control the solar water pumping system in the field. The communication system is an IoT-based SCADA using Raspberry pi Zero, Arduino Nano, a 3G module SIM 5320A, and several sensors.

Finally, the conclusion and future work is explained.

Chapter 2 Literature Review

Parvaresh Rizi et al. [8] presented a comprehensive financial comparison between different water pumping systems for which the analysis was based on the life cycle cost (LCC) method. Their discussion involved grid-connected electrical and diesel pumps, solar-powered pumps with a battery storage system, and without any storage system. The LCC comparison between solar water pumping, grid-connected and diesel pumps showed that they could be better than the other one based on different factors such as system size, government policies, etc. Also, they argued that a solar-powered pumping system in irrigation is worth more studies and investment to be considered in Iran, where the main source of energy is from limited fossil fuels mostly because it uses clean and renewable energy. In their study, they showed that using battery storage in solar water pumping reduces the size of the system, which consequently results in a lower cost. Overall, they claimed they presented all the parameters that are effective in the financial analysis of a pumping system though the details of cost analysis is not stable in Iran's market, and it is difficult to predict when it comes to using PV systems that are not manufactured inside the country. Another existing problem in their research is using any analysis tool for sizing their systems, such as for irrigation requirement analysis. Also, the types of components are unknown in their research.

Ghasemi-Mobtaker et al. [9] did a comprehensive investigation on the application of the photovoltaic system in irrigation and cultivation of a 100 ha barely field. They considered 27 samples of researches on the systems used in the irrigation and cultivation of various crops around the world and discussed that the use of traditional methods in irrigation, such as flood irrigation using diesel pumps, causes severe environmental damages. Afterward, they calculated the electrical demand for two types of irrigation of barely, surface irrigation and sprinkler irrigation, and designed a pv system using TRANSYS software that supplies the demand and analyzed the energy, environmental life cycle assessment, and cumulative exergy demand of those systems. Although their research and its findings are remarkable, the data for water requirement analysis of barely was collected from the existing farm's traditional irrigation method, which reduces the accuracy of the consequent analyses and can result in a massive difference on a large scale field (i.e., 100 ha). This critical problem can be resolved using a trusted scientific method from agricultural studies such as CROPWAT, a tool introduced by the Food and Agriculture Organization (FAO) to calculate water requirement and irrigation of crops based on soil, climate, and crop data. Also, the authors discussed that there exists a significant lack of studies that need to be done over different aspects of renewable energy systems application in irrigation in Iran.

However, in the presented study, a complete water requirement analysis for irrigation of the grape garden was done using the FAO CROPWAT tool that results in high crop yield and accurate load sizing. Afterward, the study discusses design and analysis and financial comparison of three scenarios for solar water pumping, storage less system, with battery storage system, and with a water tank system. Also, this research used and presented the products that are available in the current market.

In [10], the authors presented a low-cost open source SCADA system to monitor and control a solar system where a customer can log-in to the dashboard and apply controlling over their solar system. They used a raspberry pi, an ESP32, a WiFi router and a few sensors. Also, they used thinger.io as their design hub. This system is only implementable in places where a WiFi is available also they are using a paid IoT hub named Thinger.io which adds up to the total cost of the system. We are advancing their system by adding a cellular network modem to make it possible to implement such system in remote areas and the designed project is programmed and secured completely on the local server using Node-RED.

In [11], the authors designed a home automation system which shares a lot of similarities with the common IoT SCADA system. In their work, they made use of a raspberry pi, Arduino uno, and relays to implement controlling and monitoring through a dashboard. While this proposed system was successfully able to control the IoT devices, it uses Dataplicity to secure and expose the server to the internet which is a third-party application and puts a high risk over the server that data might be accessed through third-parties. Besides, their proposed system is not able to connect through a cellular network and is only available in urban areas. In our system, we are using NGINX to secure and proxy pass the IP requests to the server and a 3G modem to connect to the cellular network.

Lastly, it should be mentioned that there is not enough research available and the data used in this area is not enough and full details of any system are not known.

The objectives of this research are as follows:

- Site data collection
- System design with and without storage
- Dynamic modelling and simulation
- IoT-based SCADA system design and demonstration

Chapter 3 System Sizing and Modelling

3.1 Irrigation Requirement and Analysis

3.1.1 Irrigation Requirement

Analysis of the grape garden's water requirement is the most critical step in sizing such a system for micro-irrigation. A complete and correct analysis can result in higher crop yields and water savings. In this project, a complete water requirement analysis was done using Cropwat software introduced by the Food and Agriculture Organization (FAO); it is a tool for calculating several crops' water and irrigation requirements based on several factors such as soil climate and crop information. [13]–[16]

Simulation settings in CROPWAT tool:

- Climate data such as rain and irradiance were extracted using the FAO CLIMWAT tool from Urmia station. [17]
- Crop info was selected table grapes, defining different growing stages as the initial (20 days), development (50 days), midseason (75 days), late-season (60 days),

which results in a total of 205 days. Also, the planting date in that area was selected to be Mar 21.

- Soil type was selected medium (loam).

After completing these steps and settings, the CROPWAT software calculated the field's irrigation requirements, and the results are presented in Table 3.1. FAO Irrigation and Drainage Paper No. 56 can be used as a reference for a more in-depth explanation of the procedure of the analysis of crop evapotranspiration. [18]

3.1.2 Total Dynamic Head Calculation

The groundwater level in the area is 22 meters. Moreover, water pressure required at the main pipeline for micro-irrigation is considered 30 PSI, equal to 21.1 m of the head. Therefore, the total dynamic head to use in pump sizing was considered 43.1 m.

Table 3.1: Irrigation requirement results of the garden

Month	Decade	Crop Evapotranspiration (ETc) (mm/dec)	Effective rain (Eff.) (mm/dec)	Irrigation. Requirement (Irr. Req.) (mm/dec)
Mar	1	6.8	16.4	0
Apr	1	7.4	17.4	0
	2	10.7	18.4	0
	3	15.5	17.1	0
May	1	21	16	5
	2	27.4	15.2	12.2
	3	39.6	11.8	27.8
June	1	42.6	7.5	35.1
	2	47.3	4.1	43.2
	3	48.7	3.2	45.5
July	1	50.3	2.3	48
	2	52.2	1	51.2
	3	55.6	0.9	54.7
Aug	1	48.6	1	47.7
	2	45.9	0.8	45.1
	3	42.6	0.9	41.7
Sep	1	32.2	0.4	31.8
	2	26.4	0.1	26.3
	3	20.1	3.4	16.7
Oct	1	14.6	7.7	7
	2	1.1	1.1	1.1
Total	**Annual**	**656.6**	**146.7**	**540.1**

3.2 SYSTEM DESIGN

Three types of systems were proposed and discussed in this paper. Figure 3.1, Figure 3.2, and Figure 3.3 show three schematic diagrams of different equipment used in solar water pumping. These systems are discussed later in this paper. In Figure 3.1, the solar energy is directly converted to electricity using PV arrays and consumed by the motor to pump water directly into the drippers without any storing option. Here in this Fig., the controller block provides a feature to implement maximum power point tracking (MPPT), scheduling the daily irrigation, etc. In Figure 3.2, the generated electricity during a sunny day can be stored in the battery bank and consumed over a more extended period during day and night for pumping water into the drippers. In this Fig., the controller block provides the feature to implement MPPT, battery charge controller, scheduling daily irrigation, etc. In Figure 3.3, the generated electricity is consumed directly by the water pump to store pumped water into the elevated water tank used for gravity-fed irrigation. Also, the controller block acts like the one in Figure 3.1.

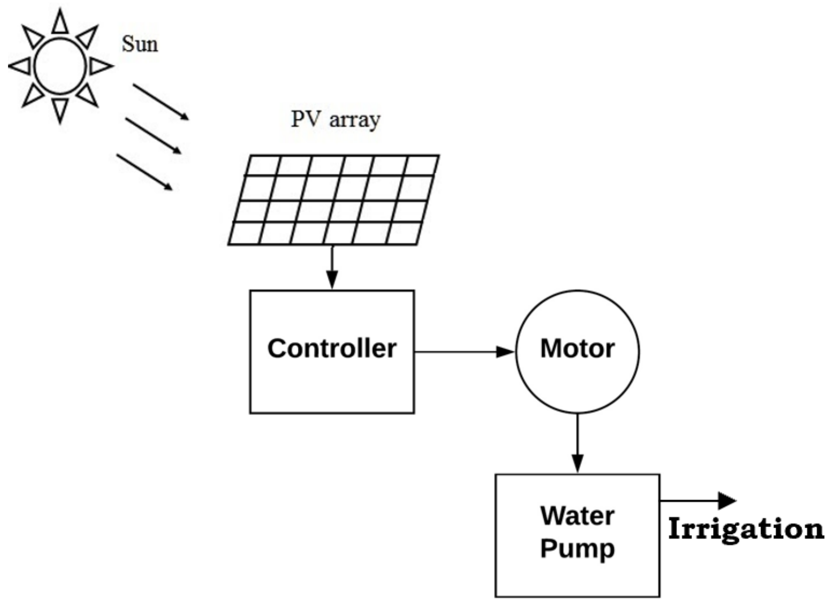

Figure 3.1: Schematic diagram of the system without any storage system

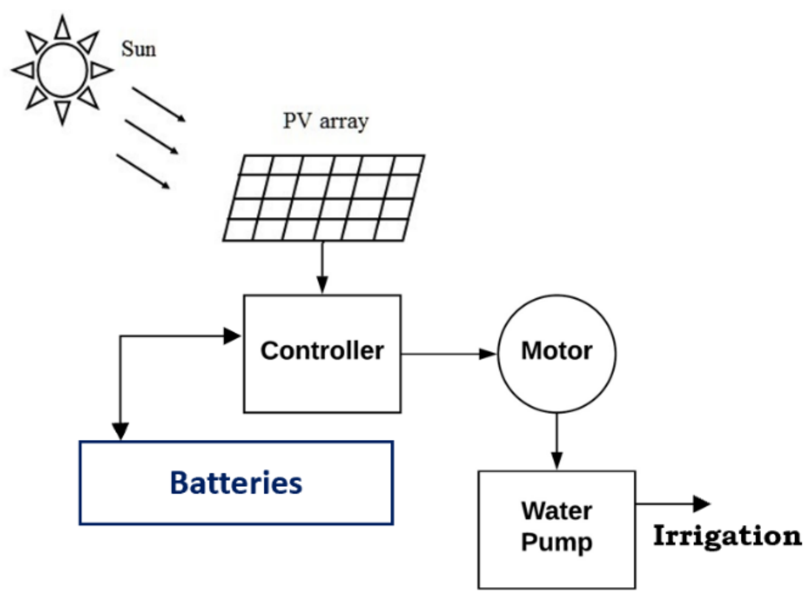

Figure 3.2: Schematic diagram of the system with a battery bank

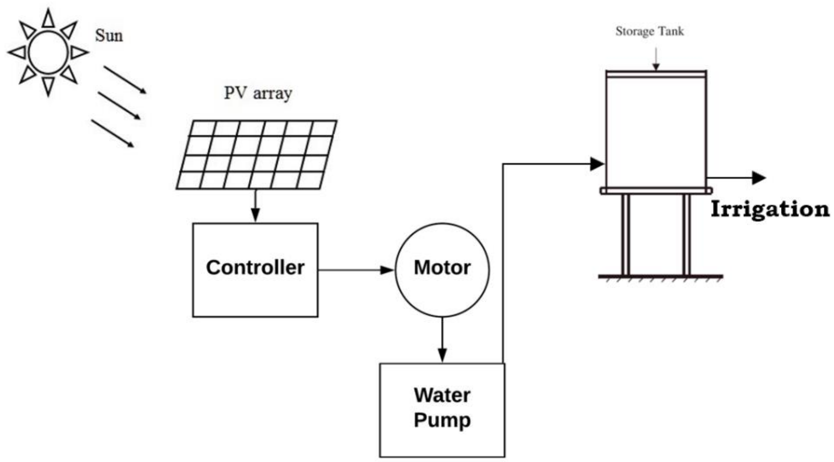

Figure 3.3: Schematic diagram of the system with a water tank

3.2.1 System A: Solar Water Pump Without any Storage

In this design, solar energy converted to electricity through PV modules is directly consumed by the submersible pump.

Lorentz Compass 3 planning and simulation tool was used to design the system, which Lorentz introduced that allows users to design solar pumps using many different types of PV and pump systems available in their company.[19]

Simulation settings in optimization with Lorentz Compass 3:

- Location: Iran, Urmia (37° North, 45° East)
- Total dynamic head: 43.1 meters

- Required daily output: 755 m^3 and sized for July (max irrigation requirement selected according to Table 3.1)

- Dirt loss: 5%; motor cable: 100m; water temperature: 20°C.

The recommended system design by Lorentz Compass3 software after optimization is as follows:

- ✓ Submersible pump model: PSk2-25 C-SJ95-4, including a 25 KW controller, 18.5 KW, 380Vac motor, and a pump. More information and datasheet available in [20].

- ✓ PV system: 36.08 KW rated capacity (16 per string x 11 string in parallel) using LC205-M72 205w High-efficiency PV Module

- ✓ Accessories: Well Probe, Well Probe V2, Float Switch, Pressure Switch, Liquid Level Sensor, Liquid Pressure Sensor, Water Meter, 3x PV Disconnect 1000-40-5, PV Combiner 1000-125-4, PV Protect 1000-125, Sacrificial Anode for 6" motors, SmartPSUk2, SmartStart, Surge Protector2

Figure 3.5 shows a photograph of the submersible pump system from Lorentz Compass3. Figure 3.4 shows the detailed simulation results for system design A. It shows daily and hourly variations of generated energy from PV panels, irradiation, rainfall, ambient temperature. As it is clear from this figure, in July, the system's maximum pumping capacity is enough to support the irrigation requirement. The results shown in this figure are the system's capability and can be modified to program the pump controller based on the irrigation requirement.

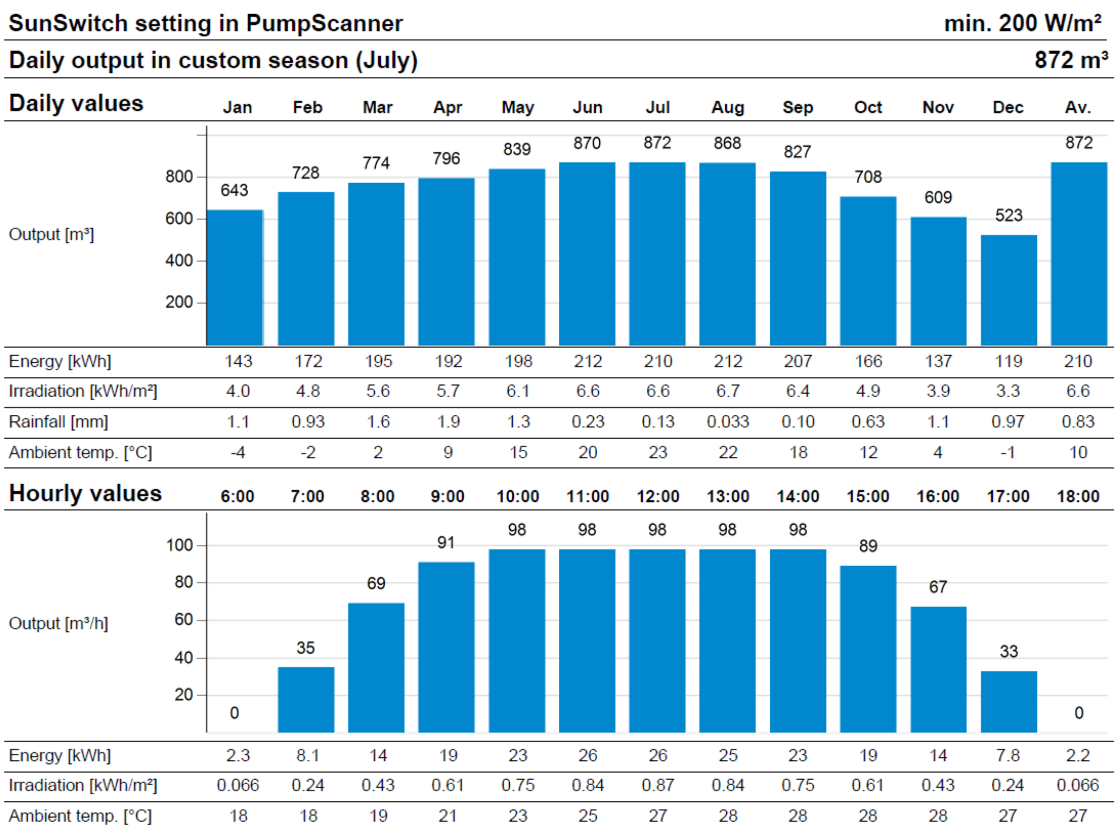

Figure 3.4: Detailed simulation results from Lorentz Compass 3 for system design A

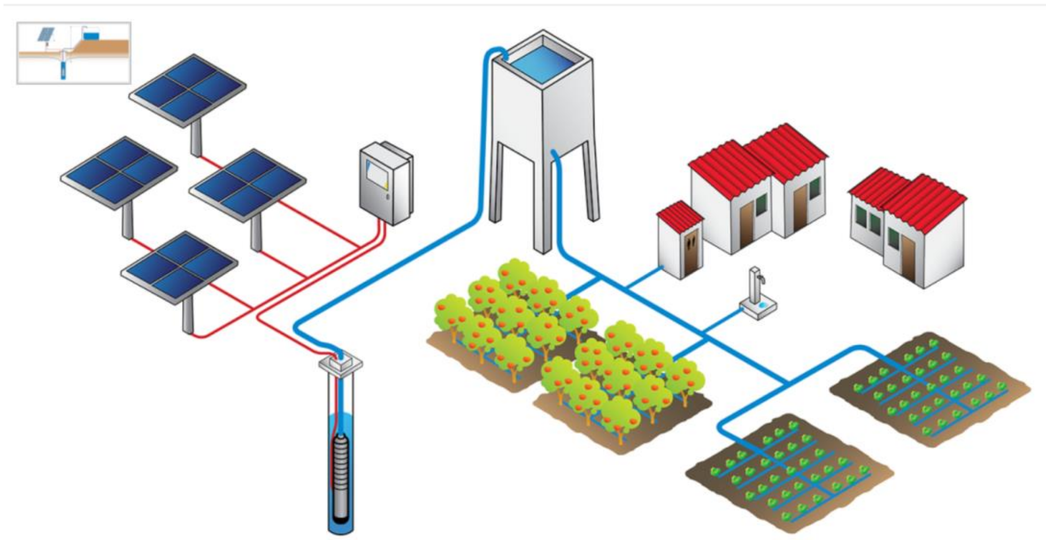

Figure 3.5: System diagram from Lorentz Compass 3

3.2.2 System B: Solar Water Pump with a Battery Bank

In this system, the use of a battery bank in designing a solar pumping was studied. Two factors need to be considered to size the load and select a pump: total dynamic head, which was calculated 43.1 meters, and water flow rate. It should be noted that the design of a battery storage system should be such that it can, alongside the PV panels input, support the supply of one day worth of irrigation. Based on that, the water flow rate was decided to be 35 m^3⁄h. Moreover, the total irrigation requirement of various months was divided by this number to give the load's hours of operation. The results are shown in Table 3.2.

Table 3.2: Daily operation hours of the pump

Month	Average hours	Round Hours
May	5.81	6.00
June	17.36	17.00
July	20.89	21.00
August	18.32	18.00
September	10.50	10.00
October	3.47	3.00

Based on the two factors mentioned earlier in this section, using pump charts of various submersible pumps in the Lorentz Compass3 tool, a 6-inch 11KW pump named Lorentz PSk2-15 C-SJ42-6 was selected. As shown in Figure 3.6, the pump chart, this submersible pump model consumes about 8.2 KW power to supply the irrigation requirements with proper flowrate and total dynamic head. It also shows that the efficiency of the pump is about 52 percent. Figure 3.7 shows a diagram of the pump system from Lorentz Compass3. More information on this pump is available in [21].

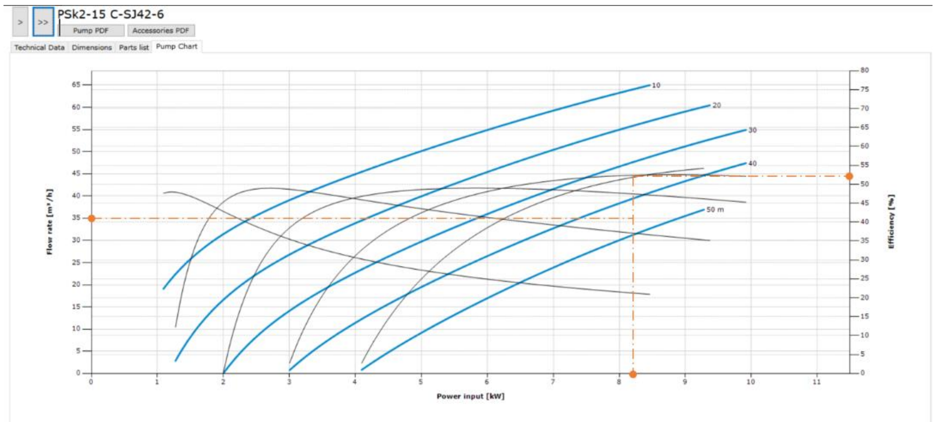

Figure 3.6: Lorentz submersible pump chart used in system B

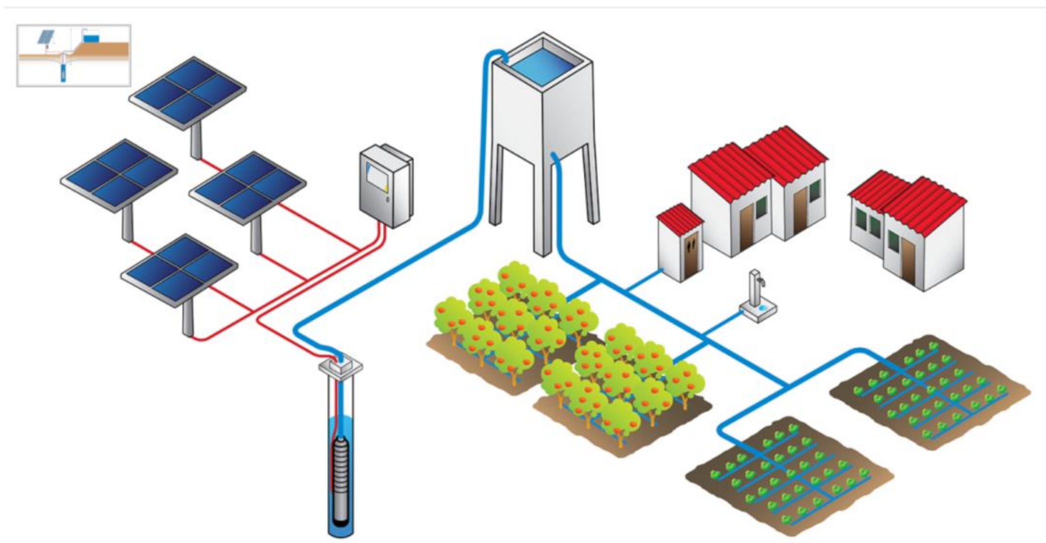

Figure 3.7: System diagram from Lorentz Compass 3

The system was optimized using HOMER Pro, software for hybrid optimization of multiple energy resources, and the system diagram is shown in Figure 3.8. This software analyses the system and considers different combinations of component sizes that meet the project's electrical constraints and proposes the most economical model based on the component costs.[22]

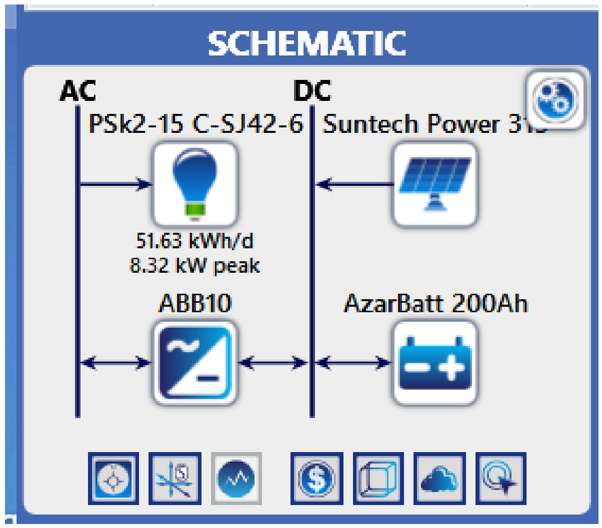

Figure 3.8: Schematic of system B in HOMER

Simulation settings in HOMER Pro:

- Location was selected Urmia, and the climate and irradiance data was extracted from NASA Surface meteorology and Solar Energy resource

- AC electrical load profile is presented in Table 3.3, and its day-to-day random variability was entered to be 0.5%.

Table 3.3: AC electrical load profile used in HOMER Pro optimization

Month	Total operation hours (h)	Start time	End time	Load size (KW)
May	6.00	11 AM	5 PM	8.2
June	17.00	4 AM	9 PM	8.2
July	21.00	2 AM	11 PM	8.2
August	18.00	3 AM	9 PM	8.2
September	10.00	9 AM	7 PM	8.2
October	3.00	12 PM	3 PM	8.2

- Battery bank: Azar Battery 12 V 200 Ah, cost (81 CAD)[23]
- Bus voltage: 360 V
- PV panels: Suntech Power315, cost (177 CAD), derating factor (85%), and with DC output [24]
- Inverter: ABB PVI10.0 I OUTD-x-US-480, cost (5,096 CAD), efficiency (97%), lifetime (15 years)
- Other inputs (project lifetime: 20 years; discount rate: 13%; inflation rate: 17%; annual capacity shortage: 0%)
- Constraints (maximum annual capacity shortage: 0%; minimum renewable fraction: 0%) and operating reserves (load in current time step%: [0, 1, 5]; annual load peak%: [0, 20, 50, 100]; solar power output %: [0, 5, 10]; wind power output%: 0)

As mentioned above, the Homer Pro optimization method was selected for sizing the system with the simulation settings. After the simulation, it was reported that 4,720 solutions were simulated, among which 1,862 were feasible, and 2,858 were infeasible due to the capacity shortage constraint. Also, 1,296 solutions were omitted due to infeasibility and no sources of power generation. Finally, the system architecture shown in Table 3.4 was selected based on the final minimum cost in HOMER Pro.

Table 3.4: System architecture resulting from the optimization

Component	Name	Size
PV	Suntech Power 315STP315-24/Vdx	44.4 KW
Storage	Azar Battery 12v 200A	60 units (2 strings)
System converter	ABB PVI-10.0-I-OUTD-x-US-480-y-z	10 KW
Load	HOMER load following	

Besides the system's sizing, the simulation results as presented in Figure 3.9 and Figure 3.10 clearly show that the system operates correctly to supply the irrigation requirements mentioned in table 1 throughout a year. According to Figure 3.9, the battery storage system's state of charge varies in the day of the month, depending on the monthly hours of operation. It remains constant during the months with no irrigation, and the system can be completely turned off. Also, Figure 3.10 shows the inverter's output power, which is connected to the pump.

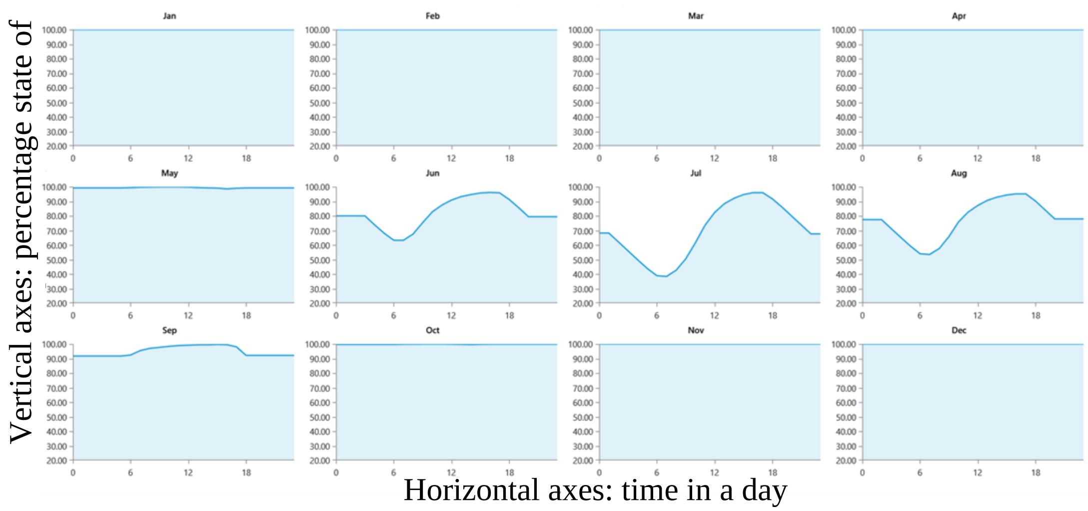

Figure 3.9: Daily profiles for various months of operation showing the states of charge of the battery storage (Azar Battery 200 Ah)

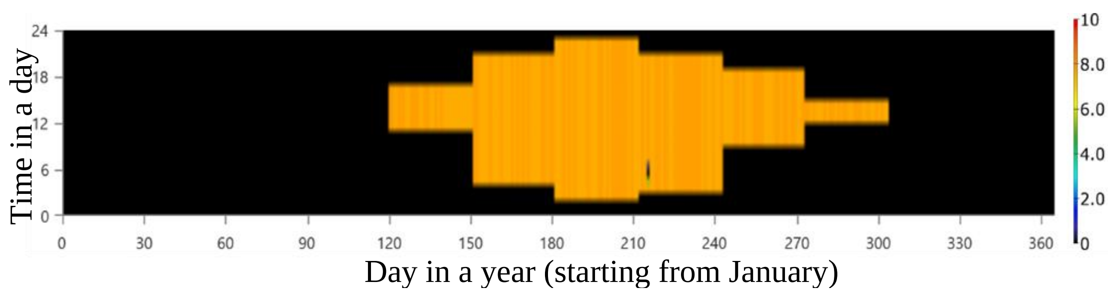

Figure 3.10: ABB PVI-10.0-I-OUTD-x-US-480-y-z inverter output (kW) throughout 365 days

3.2.3 System C: Solar water pumping with the water tank

In this design, a water tank is considered as the primary storage. First, the flowrate for irrigation is considered constant, $35m^3/h$, and it is calculated based on the average irrigation requirement. Two factors are essential: the reservoir must contain at least one day's worth of water, and it must be elevated to add constant pressure to the distribution line. Based on these two factors, the water tank capacity was calculated 800 m^3 and elevated 20 meters to ensure 15 to 30 PSI water pressure over the drippers. Figure 3.11 shows the design of the tank system. In this design, the solar pumping system's design is the same as the system without any storage to convert all the solar energy into pumped water stored in the tank during a sunny day. In the analysis of this design, a concrete-based cistern is considered the base for creating the water tank, and the concrete costs a total of 4,288.32 CAD. However, there are some high hills around the field and the tank is to be built on top of a 20m-high hill. [25]

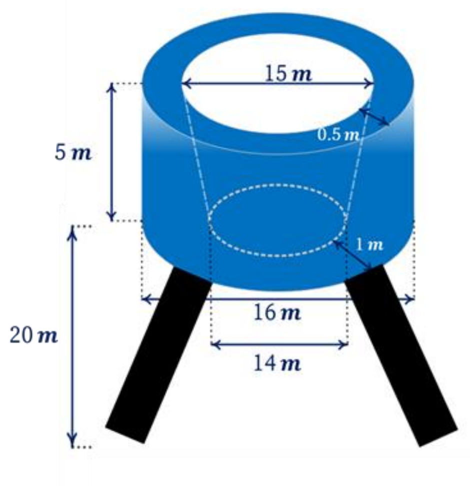

Figure 3.11: Water tank design

3.3 COST ANALYSIS

The cost of the three systems are discussed in this section and are compared to show the advantages of each system. Table 3.5 shows the list of components used in each system design and their cost. As presented in Table 3.5, the total cost of a system with a battery storage system is the minimum comparing to others. It is worth mentioning that the pipeline system's cost is also minimum when using a storage system because the water flowrate is 35 m^3/h in both types, which is much less than the flow rate in the system without a storage system. Therefore, it is economical to use a storage system with solar water pumping. Note that the components' costs are acquired from the companies, local or international, of the original items.

Table 3.5: Cost of three different solar water pumping systems ($CAD)

Component*	Without Storage (A)	With Battery Bank (B)	With Water Tank (C)
Pump system	19,934.99	15,284.68	19,934.99
Pump Controller	10,826.51	5,096.00	10,826.51
PV Panels	24,937.25	24,937.25	24,937.25
Battery Storage	N\A	4,860.00	N\A
Cistern (Concrete)	N\A	N\A	4,288.32
Total	**55,698.75**	**50,177.93**	**59,987.07**

3.4 CONCLUSION

In this project, three types of solar water pumping systems were designed and discussed. The study aims to improve crop yield by providing proper irrigation for the grape garden. For this approach, the importance of using two types of storage systems, battery bank, and water tank reservoir, were discussed, and their costs were analyzed. It was shown that a system with a battery storage system is economical. It should be noted that the total energy, electrical or mechanical, produced in these three systems is the same amount but at different rates for supplying the garden's irrigation requirement. Therefore, the return on investment factor is mainly dependent upon the initial cost.

Chapter 4 Dynamic Modeling & Control System Design

Using dynamic models allows us to simulate the real-world experiments in a computer-based program or software and extract part of their results we intend to study. Computation and mathematics are used to analyze these models and produce results of experiments. In contrast with static models which give the results at a specific time of simulation, dynamic models also allow to run the experiment and observe how the results change over time; it can be a voltage difference across a load resistor, state of charge of the battery, motor speed variation with time.

DC-DC Converters

DC to DC converters is used to convert voltage levels of a dc input to suit the required voltage of a dc load or dc link. They are highly efficient converters that use high-frequency switching in the circuit to convert voltage levels. There are several methods to increase or decrease the voltage level in dc voltages. Standard methods are using simple buck converters, boost converters, and buck-boost converters. [26], [27] A buck converter, shown in Figure 4.1, decreases the voltage level across the converter inputs and outputs. The ratio of the Vout and Vin is defined by Equation 1. [28], [29]

$$Vout = D * Vin \tag{1}$$

Vout is the converter's output voltage, Vin is the converter's input voltage, and D is the duty cycle of the converter and is a value from 0 to 1. As it is clear, the output voltage is usually less than or equal to the input voltage considering the converter's duty cycle.

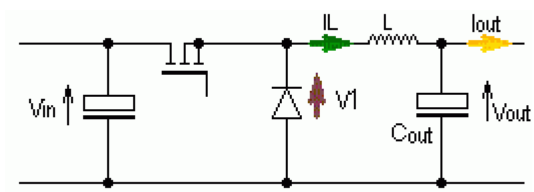

Figure 4.1: Buck converter design

A boost converter shown in Figure 4.2 is used to step up the input voltage and convert it to a higher output voltage. The ratio of the Vout and Vin is defined by Equation 2. [30], [31]

$$Vout = \frac{Vin}{1 - D} \tag{2}$$

Vout is the output voltage, Vin is the converter's input voltage, and D is the duty cycle of the converter and is a value between 0 and 1. As it is clear, the output voltage is usually greater than or equal to the input voltage.

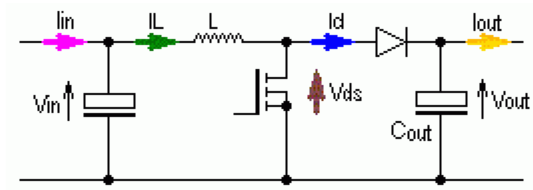

Figure 4.2: Boost converter design

A buck-boost converter shown in Figure 4.3 is used to convert a positive dc input voltage to a negative output voltage that can be greater or less than that. The ratio of the output voltage and the input voltage is defined by Equation 3.

$$Vout = \frac{-D}{1-D} * Vin \tag{3}$$

Vout is the output voltage, Vin is the input voltage, and D is the converter's duty cycle and is a value between 0 and 1. As it is clear, the amplitude of the output voltage can be less than or greater than the input voltage considering the value of the duty cycle.

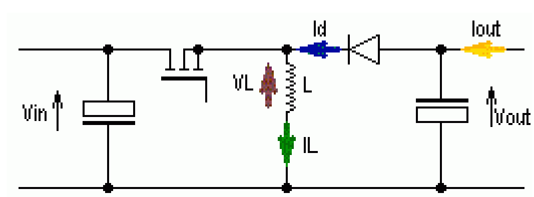

Figure 4.3: Buck-boost converter

4.1 Dynamic System Model

The general schematic diagram of the dynamic system is shown in Figure 4.4. It consists of a photovoltaic (PV) array representing PV panels arrangement; a load as the representation of the load used in the design; a battery storage system block representing the storage system's dynamics; and a control block that contains all the controlling entities of the design. It should be noted that this figure is the general schematic diagram of a dynamic system in a very simplified method.

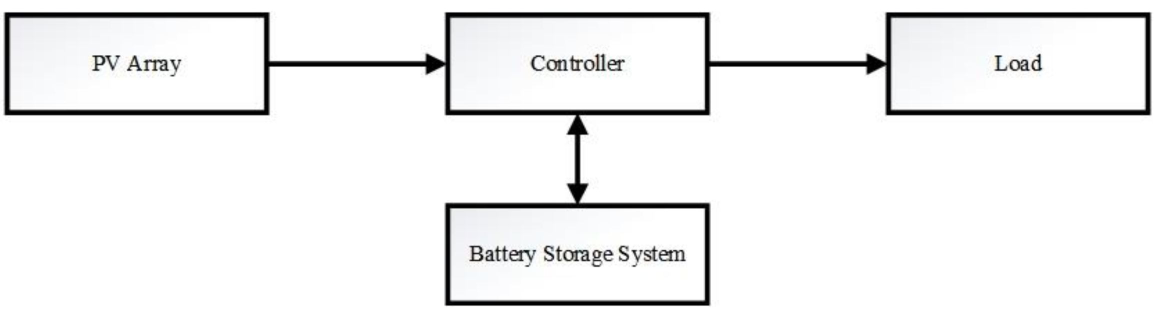

Figure 4.4: General schematic diagram of the dynamic model used in the project

A Simulink model was designed to study the presented system and is shown in Figure 4.5. In this model, a PV array is connected to a buck converter and afterward to the load. Besides, the battery storage system is connected to the dc link. A measurement unit is designed to monitor the simulation results of the system. As shown in this figure, a controller subsystem unit is also designed to arrange the model's controlling entities. Specifications and configurations of the system are discussed later in this section.

PV array

In the previous chapter, the sizing of the solar water pumping with a battery storage system was studied entirely, and HOMER Pro based results were extracted. According to the results and the arrangement presented in Table 3.4: System architecture resulting from the optimization), the PV array was selected Suntech Power STP 315-24/Vdx, and its characteristics are shown in Figure 4.6. We need to consider two factors to decide about the array data where the number of parallel strings and series-connected modules per string is input: the voltage of the dc bus and the power of the array.

From the previous chapter, it was known that the voltage of the dc bus was 360 v. Besides that, the PV modules are 72-cell, which is nominally called a 24 v module. Therefore, it was required to consider 15 modules connected in series that sum up a voltage of 360 v. [32], [33]

Also, the PV array size was optimized using HOMER Pro in the previous chapter and was calculated to be 44.4 KW. If we divide this value by each string's size, we can get the number of strings connected in parallel. 44.4 KW divided by 4.725 KW equals 9.397. Therefore, it was decided that ten strings need to be connected in parallel to provide the system's minimum power requirement.

DC-DC Buck Converter for MPPT

As described in this chapter's background section, three types of dc to dc converters can be used to control the dc voltage and connect the PV arrays to the dc link. A buck converter steps down the input voltage, a boost converter steps up the input voltage, and a buck-boost converter allows both features of the buck and boost converter to be implemented.

To decide the type of converter, we need to consider two factors: the dc bus voltage and the PV array's output voltage range. The dc bus voltage was decided in the previous chapter to be 360 volts. Moreover, the output voltage range of the PV array can be evaluated from the PV array's characteristics shown in Figure 4.6. As shown in this figure, the maximum power point voltage is 45.5 v. If we consider 15 modules connected in series, the output voltage of the PV array adds up to 682.5 v. Besides, it is known that the PV modules are 24 v modules, and considering 15 of them in series, adds up an output voltage of 360 v. Therefore, the output voltage of the array can vary from 360 v to 682.5 v.

From what is mentioned above, using a buck converter is the best way to control the output voltage of the PV array and link it to the dc bus because the output voltage of the PV array is usually higher than the bus voltage during regular operation.

Figure 4.5 shows the buck converter connected between the output of the PV array and the dc bus where the battery storage system is connected.

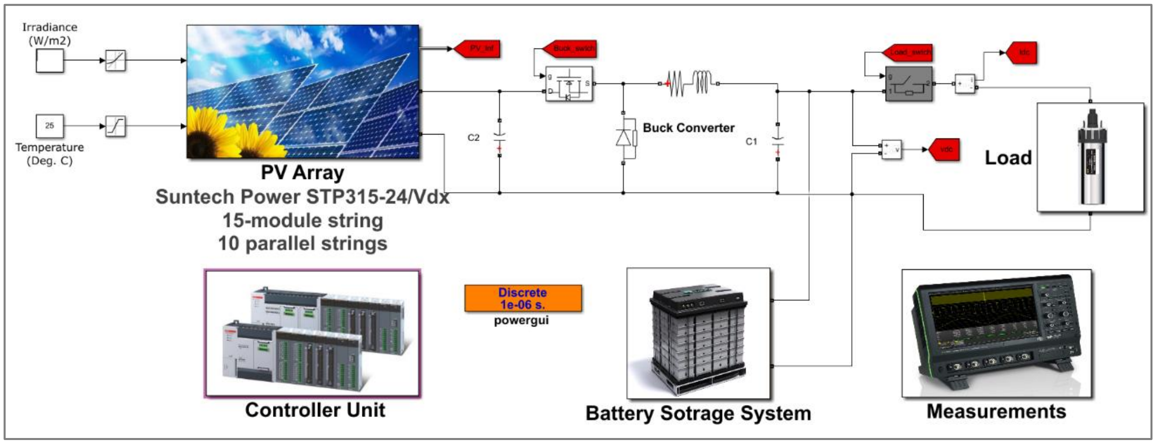

Figure 4.5: Dynamic system design in MATLAB/Simulink

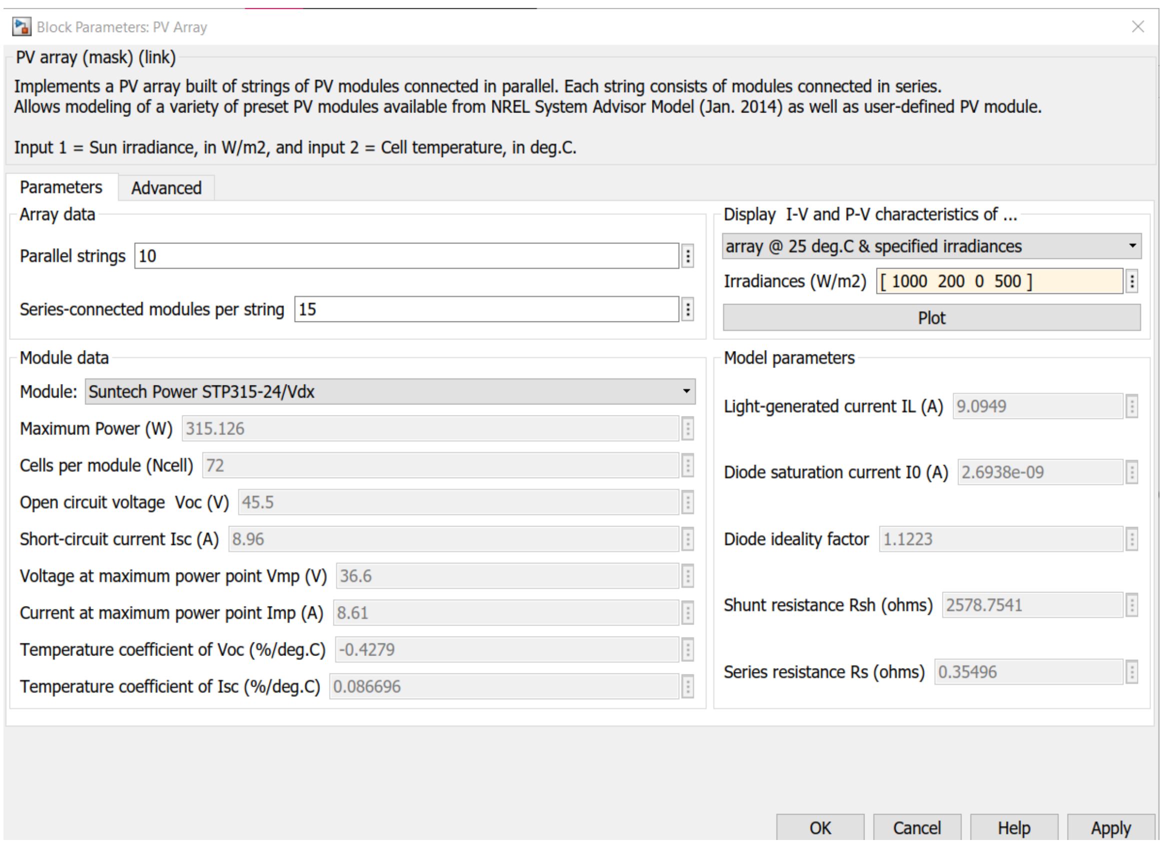

Figure 4.6: Characteristics of the selected PV array in MATLAB Simulink

The buck converter's design was done using reference [29], and the details are presented in Table 4.1. In this table's input rows, Vin_min and Vin_max are minimum and maximum input voltages, Vout and Iout are output voltage and currents, f is the switching frequency, and Vin is the sample input voltage for calculating a sample result showing the behavior of the converter. In this table's output rows, L is the inductor's value to be used in the converter, and ΔI_L for V_{in_max} is the inductor current variation at the maximum input voltage. However, it should be noted that the PV array's output power is not constant relative to the voltage variation. Therefore, ΔI_L for V_{in_max} shown in the converter results only stands for the converter's capability, and it is not the actual behavior of the dynamic model.

Table 4.1: Buck converter design details

Inputs	V_{in_min} = 360.0V	V_{in_max} = 682.5V	f = 5.0kHz
	V_{out} = 360.0V	I_{out} = 123.33A	**V_{in} = 549.0V**
Results	L = 690.2uH	ΔI_L for V_{in_max} = 49.33A	

Considering the above characteristics in the buck converter's design, it will have the voltage and current responses shown in Figure 4.7. The output voltage was given 360 v constant, and the input voltage was given 549 v, which is the PV array's MPPT voltage.

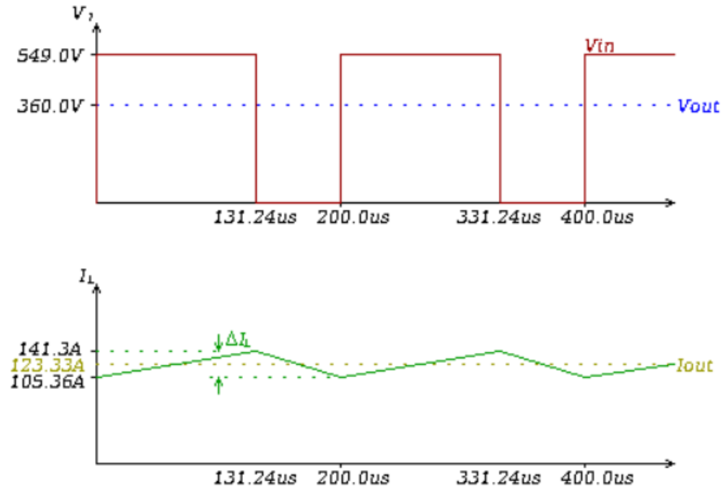

Figure 4.7: Voltage and current responses of the buck converter at Vin=549 (array's voltage at MPPT)

Battery storage system

In Figure 4.5, the block named "battery storage system" is a subsystem consisting of a lead acid battery and a bidirectional dc-dc converter operating as a charge controller, allowing the system to keep the dc bus voltage constant by charging and discharging the battery. Figure 4.8 shows the dynamic model of the battery storage system. The lead-acid battery characteristics were calculated based on Table 3.4: System architecture resulting from the optimization) and are shown in Figure 4.9 and Figure 4.10.

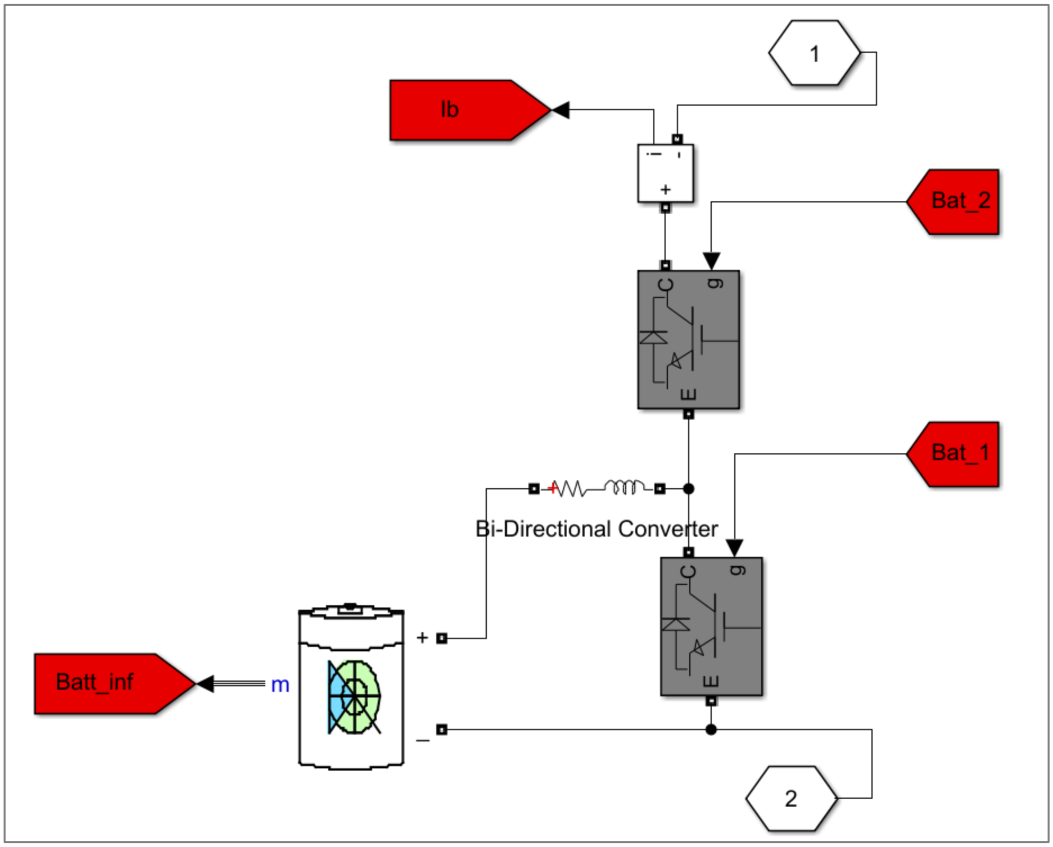

Figure 4.8: Battery storage system with bi-directional dc-dc converter as a charge controller

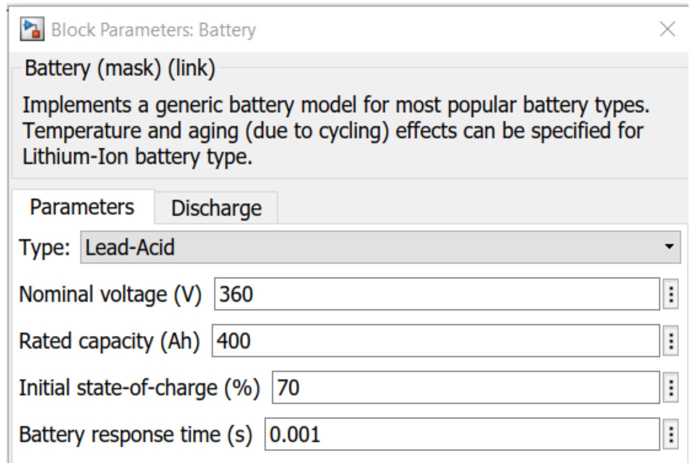

Figure 4.9: Nominal parameters of the lead acid battery

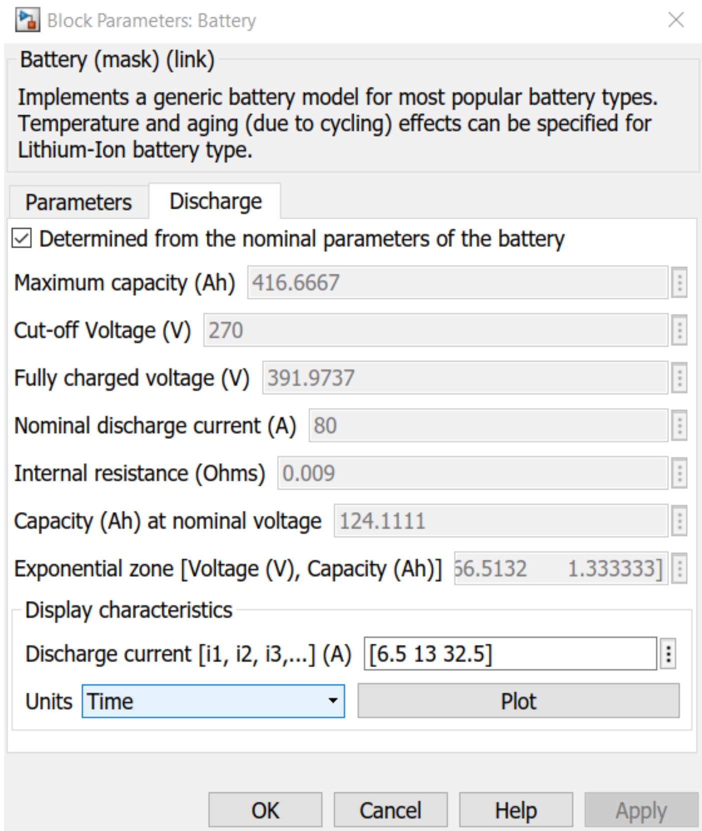

Figure 4.10: Discharge parameters of the lead-acid battery

Bi-directional DC-DC converter

A bidirectional DC-DC buck-boost converter was used to control the current flow through the battery, which consequently results in the control of the battery's charge. It is shown in Figure 4.8 and consists of two IGBT diodes and a boost inductor. In this regard, the boost inductor was calculated using the online calculator available in [34]. The calculation inputs and results are shown in Table 4.2. [35]–[38]

Table 4.2: Converter Design for bidirectional DC-DC converter

Inputs	V_{in_min} = 270.0V	V_{in_max} = 360V	f = 5.0kHz
	V_{out} = 360.0V	I_{out} = 80A	**V_{in} = 300.0V**
Results	L = 317.6uH	ΔI_L for V_{in_max} = 42.75A	

Where Vin_min is the minimum input voltage selected from the battery's cut-off voltage, Vin_max is the maximum input voltage selected based on the bus voltage and battery nominal voltage, Vout is the DC bus voltage which should be constant, Iout is the output current and is based on the battery's nominal discharge current, f is the switching frequency of the controller, and Vin is a sample input voltage for calculation are the inputs of the calculator. L is the boost inductor's value, and ΔI_L for V_{in_max} is the variation of the inductor's current when the input voltage is maximum are the calculator results.

Figure 4.11 shows the input and output voltage and current responses of the converter when Vin is 300 v. However, it should be noted that these responses only stand for the converter's capability, and the responses of the dynamic simulation can be different from what shown in Figure 4.11.

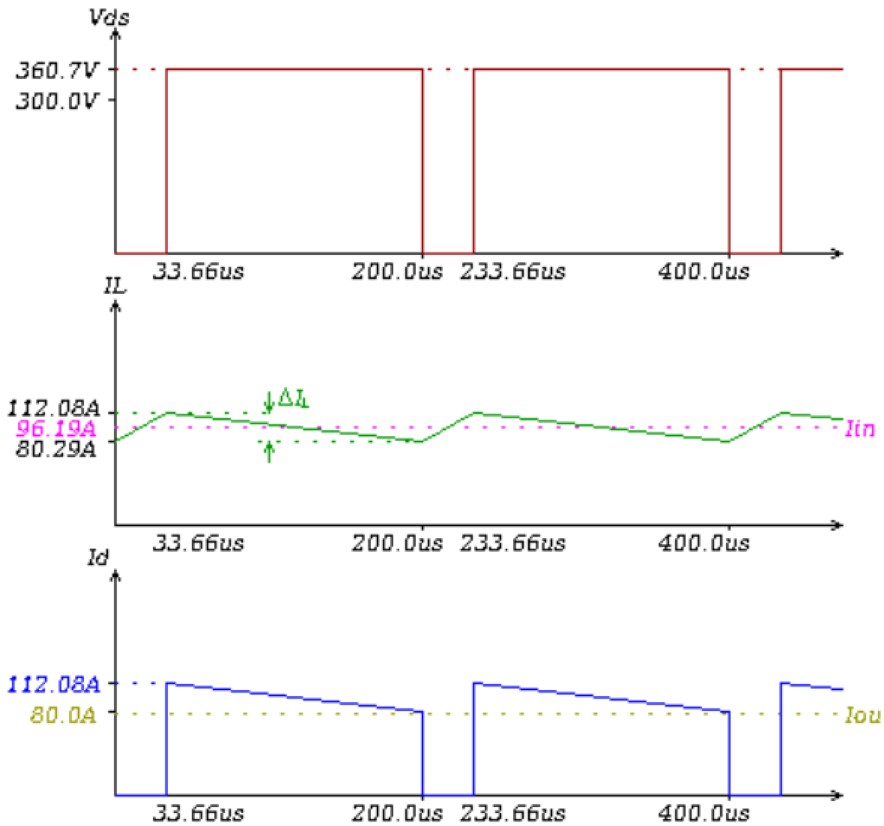

Figure 4.11: Voltage and current responses of the bi-directional DC-DC boost converter at Vin=300 (Battery Voltage)

Load

The load was selected as a resistive load representing the system's load consisting of the inverter and water pump unit at its water discharge rate. It was shown in Figure 3.6: Lorentz submersible pump chart used in system B) that the power consumed by the water pump was 8.2 KW.

4.2 Control System Design

A controller unit was designed to implement controlling topologies for the dynamic model, and it is shown in Figure 4.12. The entities in the controller unit are as follows: an MPPT controller to harvesting maximum power from the modules, a battery overcharge protection controller that can be used to protect the battery from overcharging, a load control that is used to switch off the load in order to prevent over-discharging the battery in situations that irradiance is not enough to support the load requirement and the state of charge of the battery is below the minimum, and a battery charge controller.

MPPT Controller

MPPT stands for maximum power point tracking and is used for extracting the maximum power from renewable systems such as wind turbines and solar photovoltaic modules and transfer the power to the load or store the energy. For this purpose, a dc-dc converter, a buck converter in this project, can control the voltage of the PV module. Varying the dc-dc converter's duty cycle can change the impedance of the load seen from the PV module output terminals and, consequently, the output voltage.

Figure 4.13 shows the output power and current of the PV array used in the dynamic model versus voltage at different solar irradiance values. This response was extracted from the PV array characteristics shown in Figure 4.6.

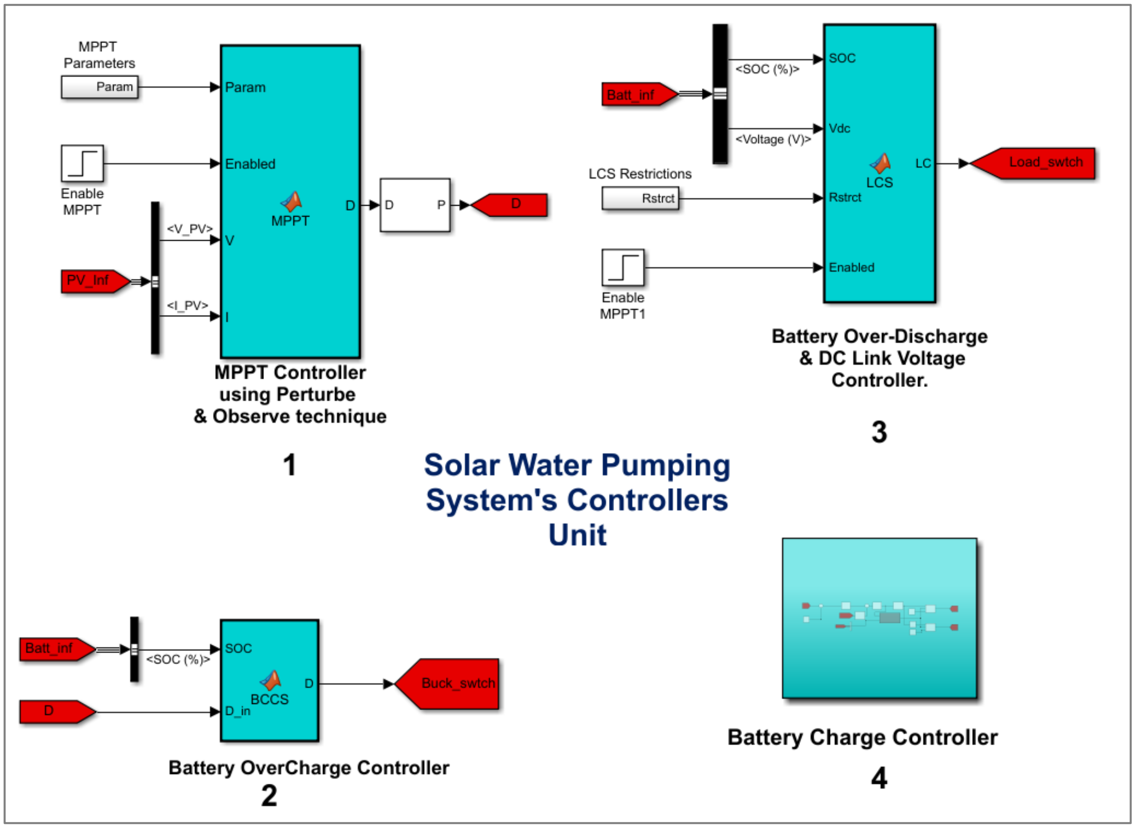

Figure 4.12: Dynamic system's controller unit

As it is clear from Figure 4.13, the power of the PV array for a given solar irradiance and temperature varies from zero to maximum relative to the voltage at its output terminals. Therefore, a controlling technique is required to extract the maximum power from the PV panel. According to Figure 4.14, controlling the voltage of the PV module allows the system to control its output power.

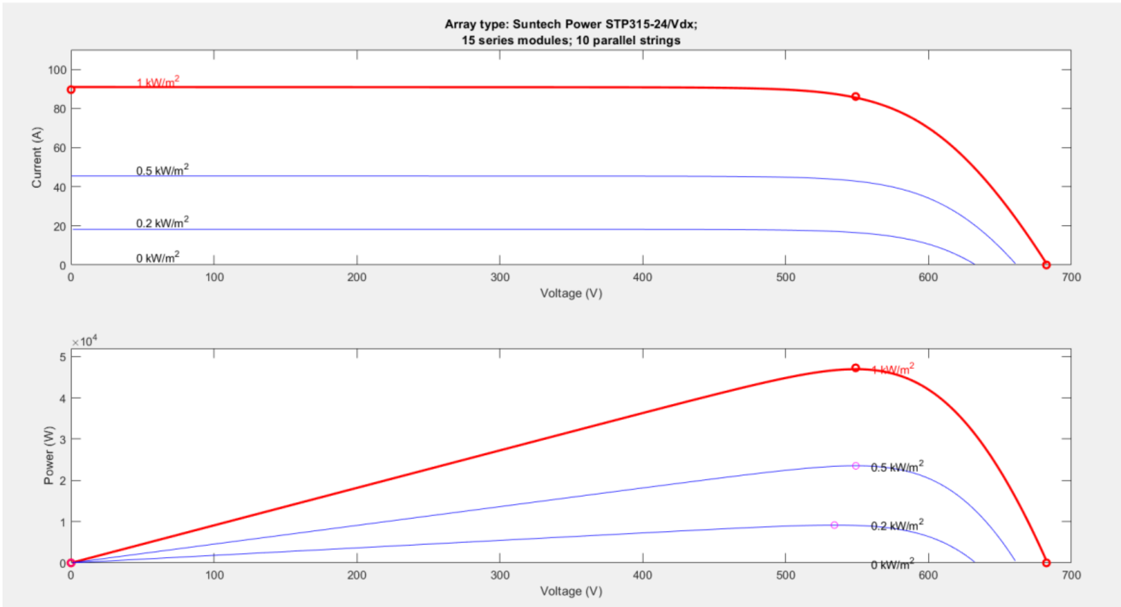

Figure 4.13: Output power and current of the PV array versus its voltage at different values of the irradiance

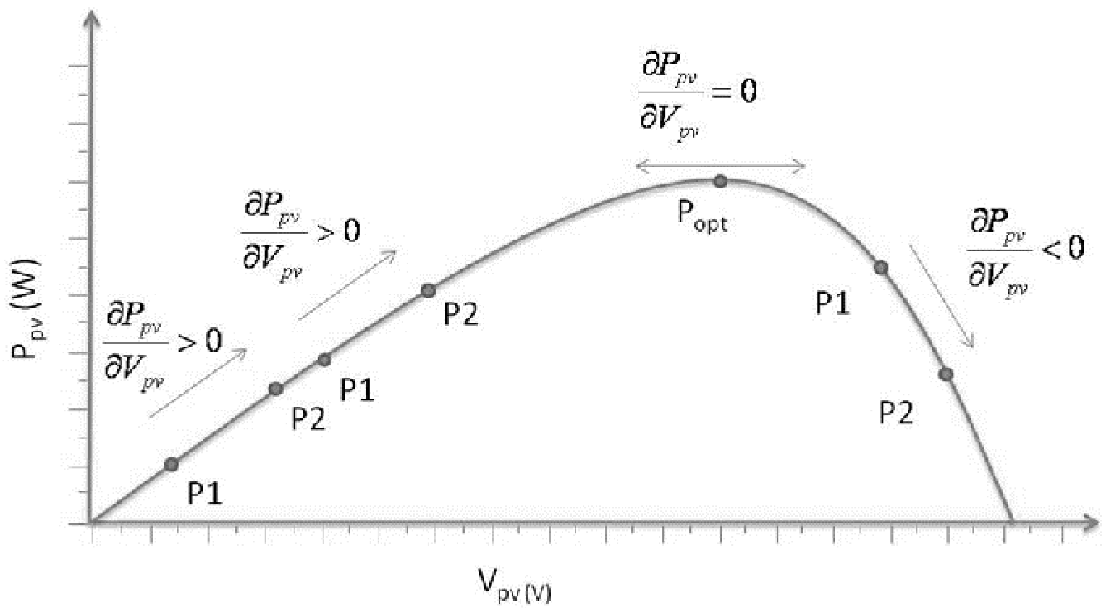

Figure 4.14: Illustration of the MPPT technique using power and voltage of the PV

There are numerous types of MPPT techniques in the literature for maximum power extraction from the PV module, such as the Curve-Fitting Technique, Look-up Table Technique. In this project, the perturbation and observation method was used to extract maximum power from the PV array. Figure 4.15 shows the flowchart of the perturbation and observation technique. [39]–[42]

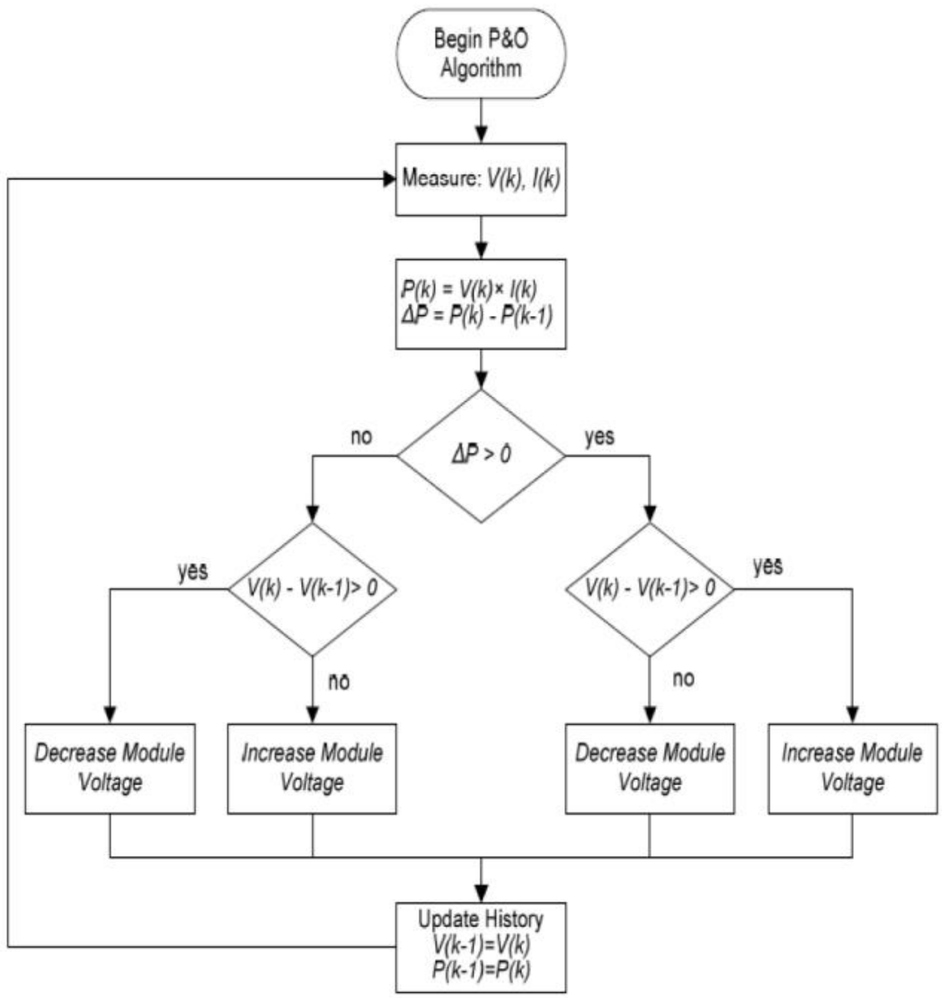

Figure 4.15: Flow chart of the perturbation & observation technique for MPPT

Figure 4.16 shows the Simulink model and function designed for MPPT, and Figure 4.17 shows the MPPT parameters. The code for the MPPT function is available in the appendix.

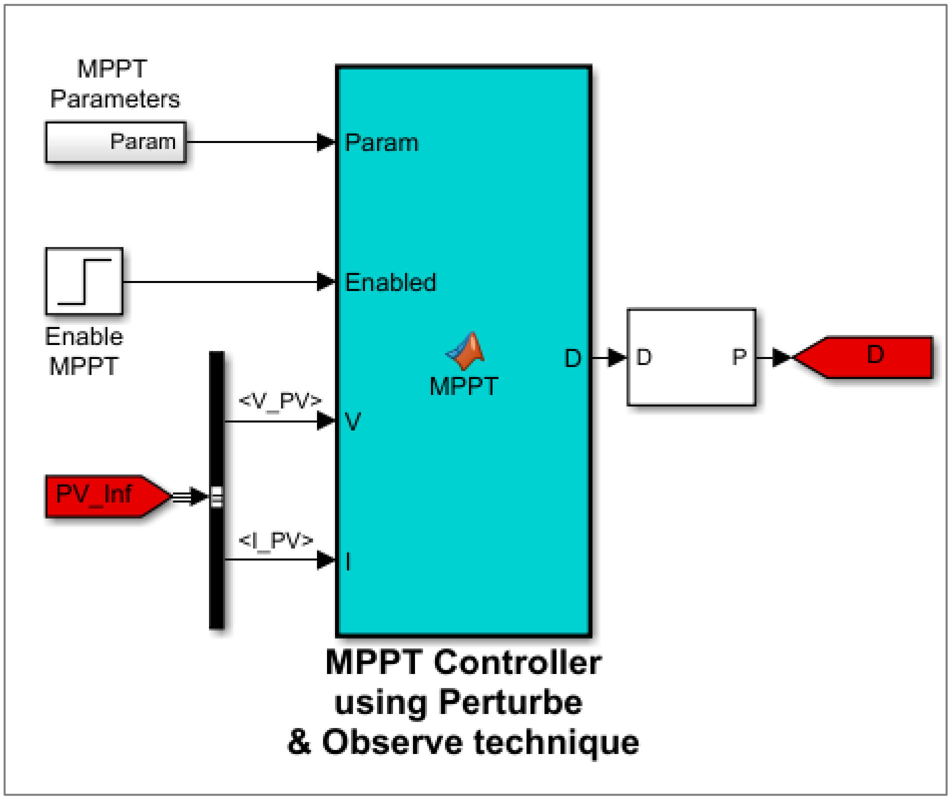

Figure 4.16: MPPT controller using Perturbation & Observation technique

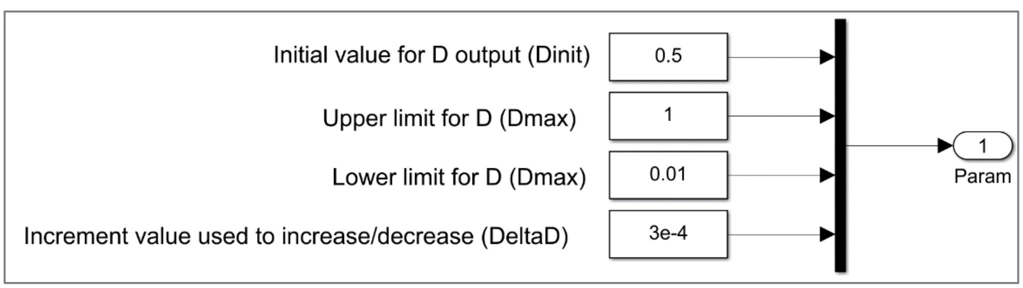

Figure 4.17: Parameters for Perturbation & Observation algorithm (D = Buck converter duty cycle)

Battery Over Charge Controller

In a situation that the generated energy from the PV array is high enough that the battery is fully charged, a controller is required to disconnect the PV array from the system to protect the battery from overcharging, which can cause severe damages to the system such as battery explosion. Figure 4.18 shows the battery overcharge controller. It takes the signal of the duty cycle of converter produced from the MPPT controller and passes it through if SOC is in an acceptable range. Otherwise, it produces zero to the buck switch to disconnect the PV array. It should be noted that the battery storage system is intended to remain connected during normal operation of the load to keep the dc bus voltage steady and reliable.

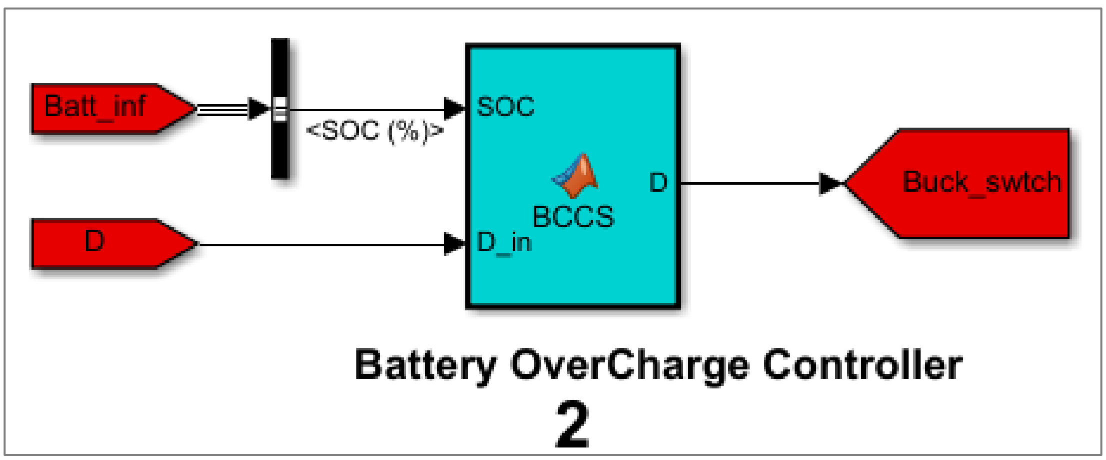

Figure 4.18: Model for battery over charge controller

Load control

To protect the industrial machines, submersible pump unit in this project, a protection system was designed. It controls the load switch and ensures that the state of charge of the battery and the voltage of the dc link is within an acceptable range. Figure 4.19 shows the model for load control.

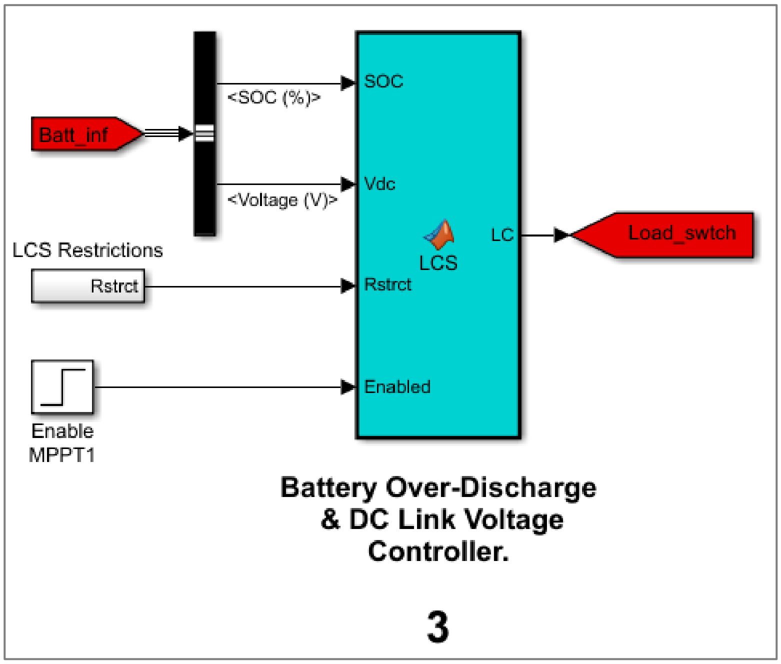

Figure 4.19: Load control unit

Battery charge controller

A battery storage system can be implemented for various purposes in a renewable energy system. In this project, the battery storage system is used to store a portion of the energy, serve the load continuously for a more extended period, and control the dc link's voltage. It was previously discussed that a bidirectional buck-boost converter was designed in dynamic modeling. Therefore, it is required to develop a robust controller to drive the battery storage system. The control system linked with the bidirectional converter is shown in Figure 4.20.

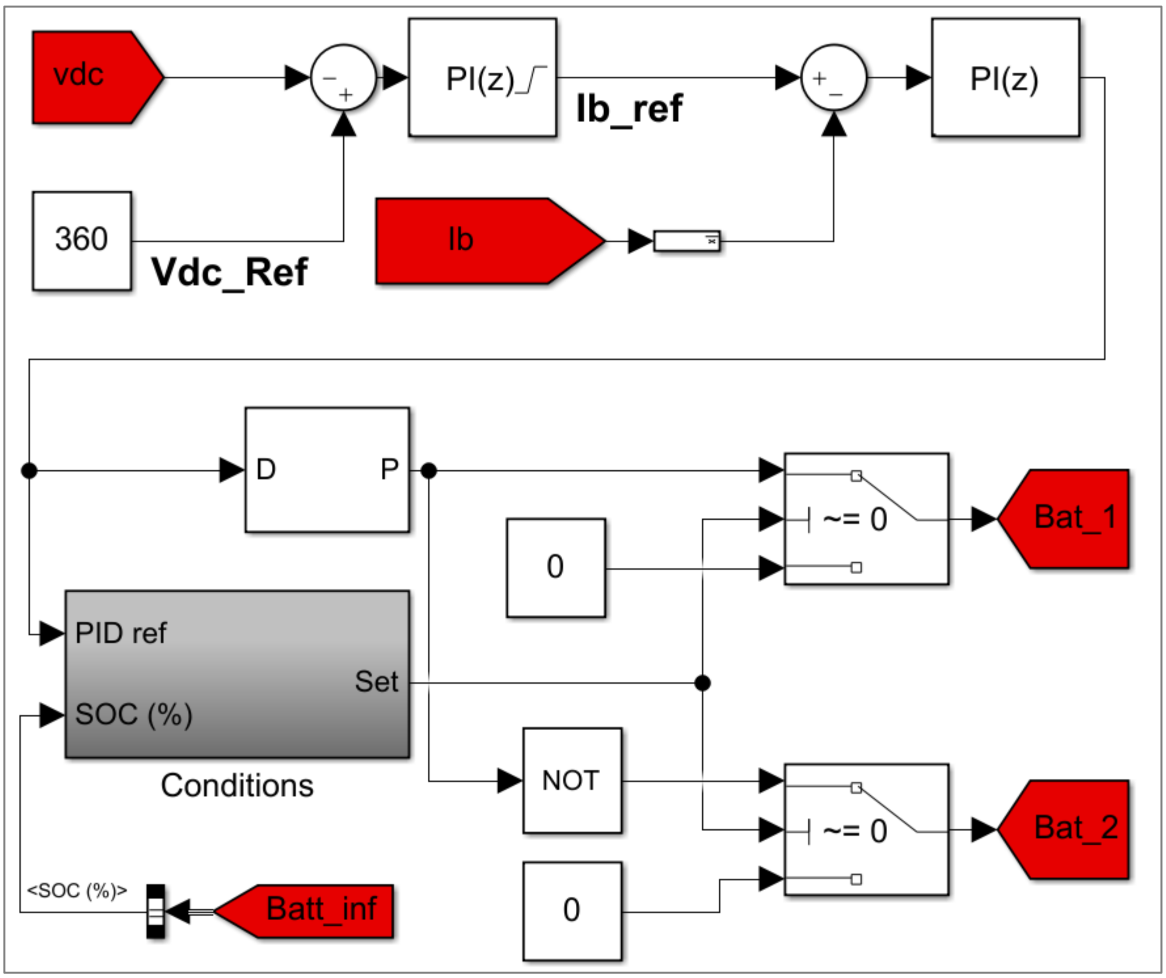

Figure 4.20: Battery charge controller

As shown in Figure 4.20, the dc bus voltage was taken and compared with a reference voltage of 360v, and then a PI controller was used to mitigate the error. The error is considered an Ib reference, the reference battery current, and is compared with the battery's actual current. Also, a limiter option was applied in the PI controller to limit the maximum error, Ib(max), to 80 A, which is the maximum discharge current of the battery shown in Figure 4.10 to ensure a safe battery operation. A PI controller was used to control the error. The error was then passed through a PWM generator to create controlling signals for the IGBT switches in the bidirectional buck-boost converter.

Besides, a condition checking block was designed to control if the SOC is within an acceptable margin and the error is not zero; otherwise, to turn off both IGBT switches.

4.3 Simulation Results

The entire solar pumping system was simulated under variable solar irradiance conditions. Since it is critical to examine the components' condition, such as their voltages and currents, a measurement unit comprised of scopes was designed and is shown in Figure 4.21. In this regard, voltage, current, and power of the system's different components were observed.

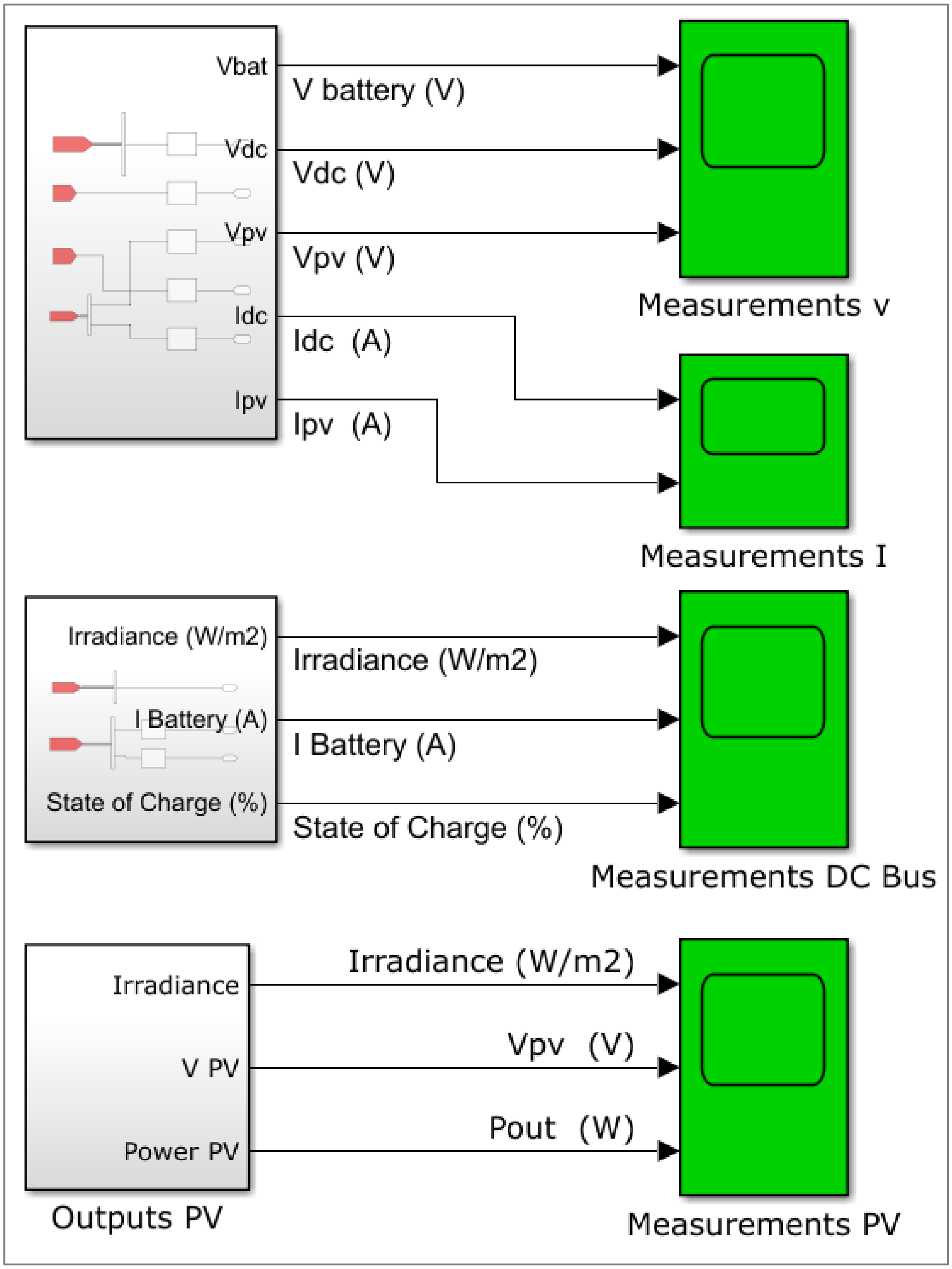

Figure 4.21: Monitoring and measurement unit

Figure 4.22 shows the graphs for the input solar irradiance, the voltage of the PV, and the output power of the PV. As it is clear from this figure, the MPPT controller was successfully able to control the voltage at the maximum power point and extract maximum power at any different solar irradiance. It should also be noted that the PV array's voltage at the maximum power point is shown in Figure 4.6 and was about 550 v.

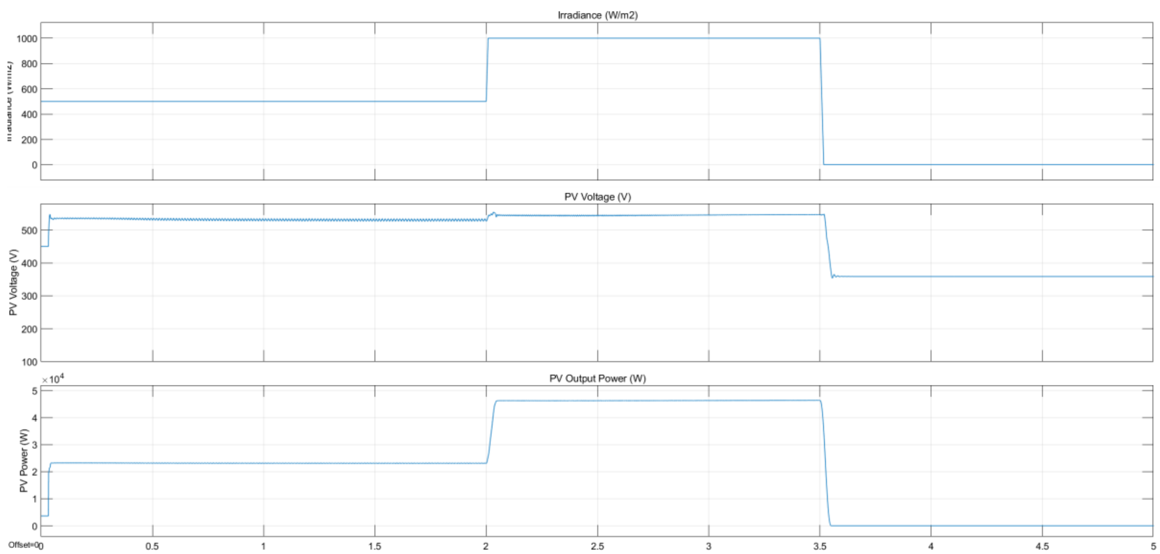

Figure 4.22: Solar irradiance, PV voltage, and PV output power

Figure 4.23 shows the graphs for the battery voltage, dc bus voltage, and PV voltage. As shown in this figure, the bus voltage was controlled and kept at around 360 v during different solar irradiance conditions and PV output. Comparing these three graphs shows that the dc-dc buck converter for MPPT and bidirectional dc-dc buck-boost converter for the battery storage system were operating correctly.

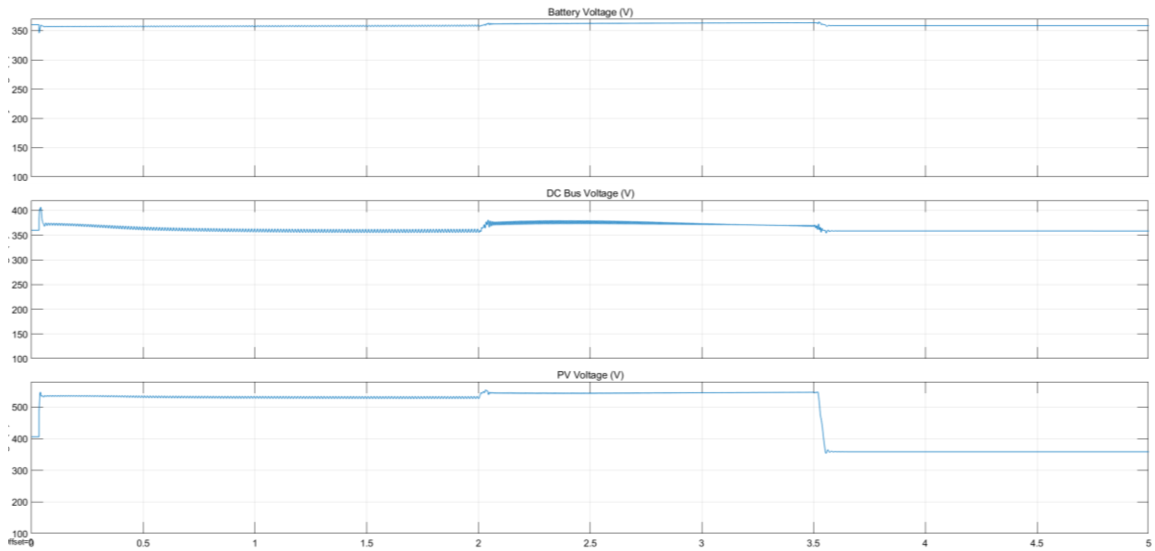

Figure 4.23: Battery voltage, DC bus voltage, PV voltage at different solar irradiance conditions

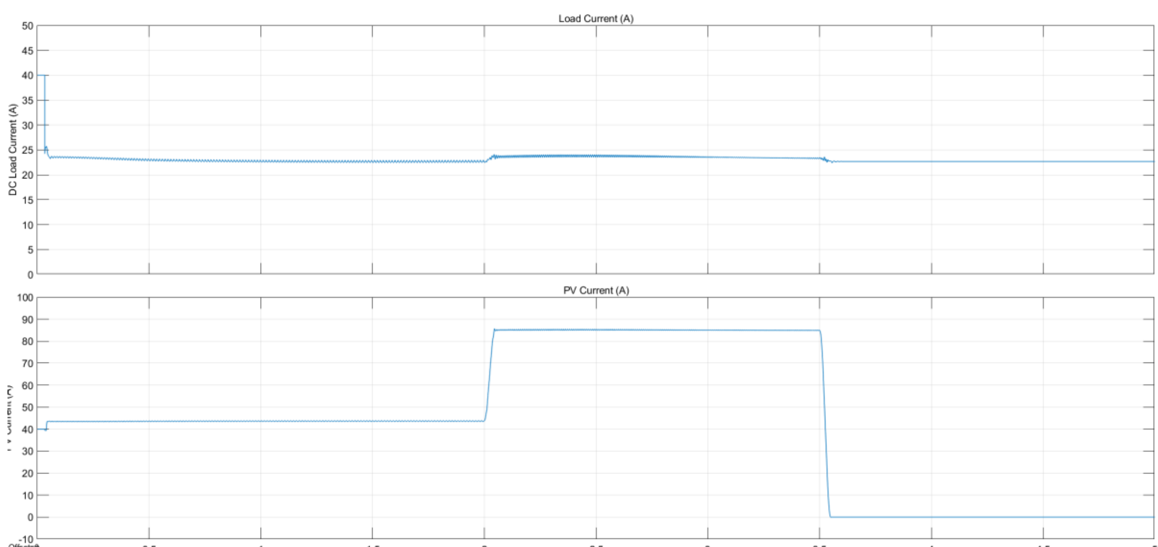

Figure 4.24: Load current and PV current at different solar irradiance conditions

Figure 4.24 shows the load current and PV current at different solar irradiance conditions. As shown in this figure, the load current is constant at around 23 A, and considering the dc bus voltage, 360 v, the load power is about 8.28 KW, which is the power of the pump unit at its rated flow for irrigation. The PV current varies from zero to 85 A during different solar irradiance conditions. It is clear from this figure that the battery storage system's operation was successful in keeping the load supplied at its reliable power requirement.

Figure 4.25 shows the solar irradiance, battery current, and the state of charge of the battery. It shows that the amplitude of the battery current varies during different solar irradiance conditions. The battery is charging to store the excess energy during the time that irradiance is available and is discharging to supply the load when irradiance is zero.

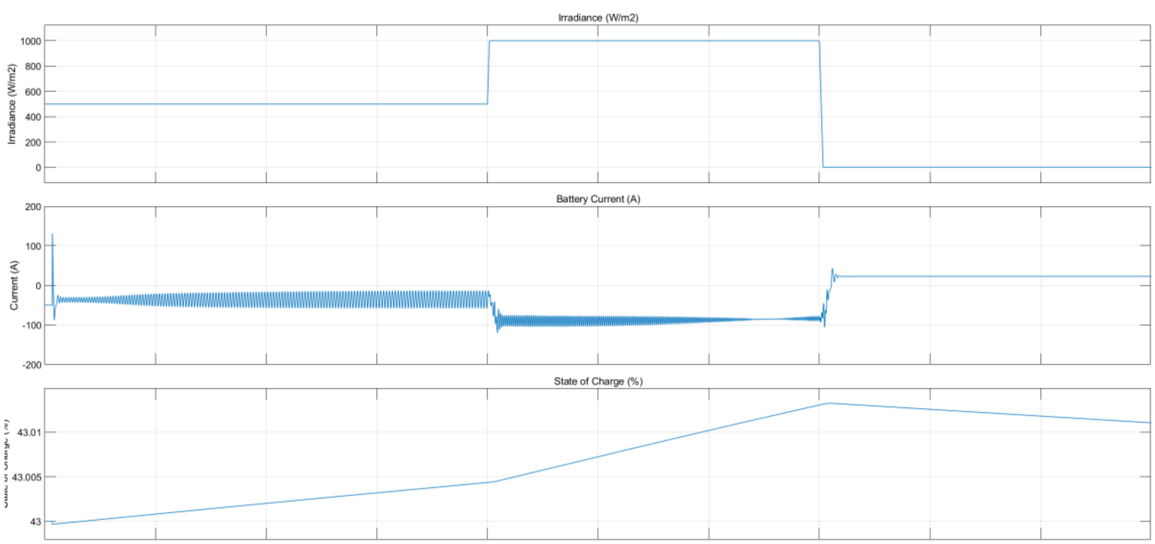

Figure 4.25: Solar irradiance, Battery current, and state of charge of the battery

4.4 Conclusion

This chapter studied the design and simulation of the solar water pumping with a battery storage system for drip irrigation of the fruit garden. The Simulink model is comprised of a PV array, battery storage system, a dc-dc buck converter, a resistive load, a controlling unit, and a measurement unit. The dc-dc buck converter was used for controlling maximum power extraction from the PV arrays, and a bidirectional dc-dc buck-boost converter was used for controlling the charge of the battery and the voltage of the dc link.

The simulation was done under different solar irradiance conditions, and the results were extracted. It was shown that the MPPT controller was successfully able to keep the PV voltage at its MPP and extract maximum power from the PV array during various solar irradiance conditions. Also, the voltage of the dc link was observed, which showed that the battery storage system was successfully able to keep its voltage at around 360 v. Furthermore, the results showed that the battery storage system was able to store the excess energy during the period that the energy generation was high and supply the load during the period that energy generation was low.

Chapter 5 Communication & Data Logging System Design

Figure 5.1 shows a schematic of a solar water pumping system. In this research, a SCADA system was developed to take various sensors such as PV voltage and current and control various switches for the submersible pump and photovoltaic panels. The SCADA also provides monitoring for the environmental parameters such as a picture of the field and solar irradiance.

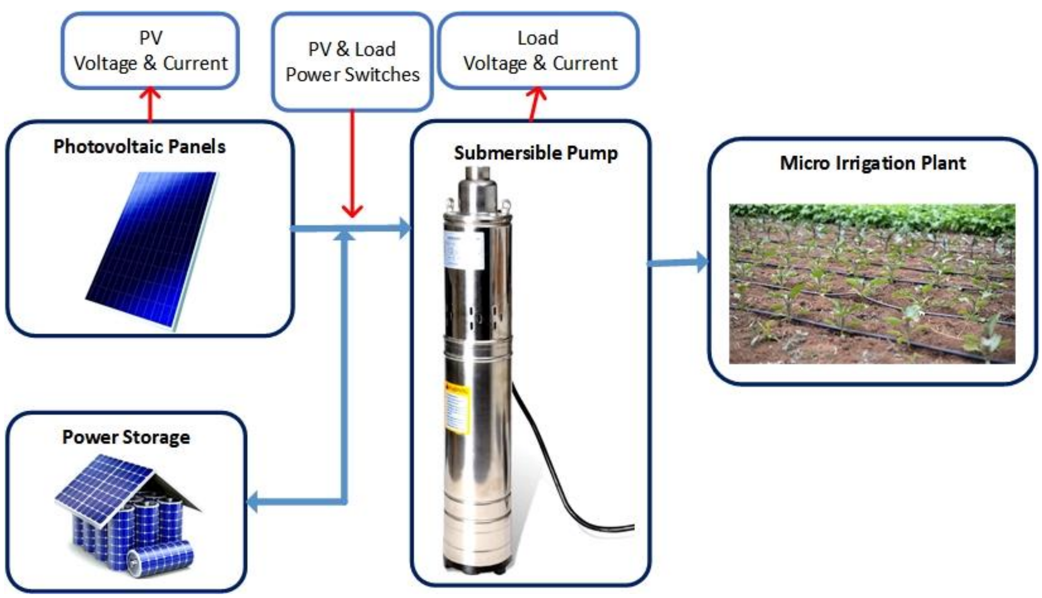

Figure 5.1: Schematic diagram of a solar water pumping system

5.1 SCADA Design

Figure 5.2 shows a diagram of the proposed SCADA system. In this diagram, an Arduino nano is connected through a USB port to the raspberry pi and allows it to control sensors and LEDs connected to the Arduino ports. Also, a camera is used to picture the crop field or pumping system to monitor them. For wireless connectivity, we used both WiFi and 3G cellular network. The design procedure and explanation of the project are included in the following.

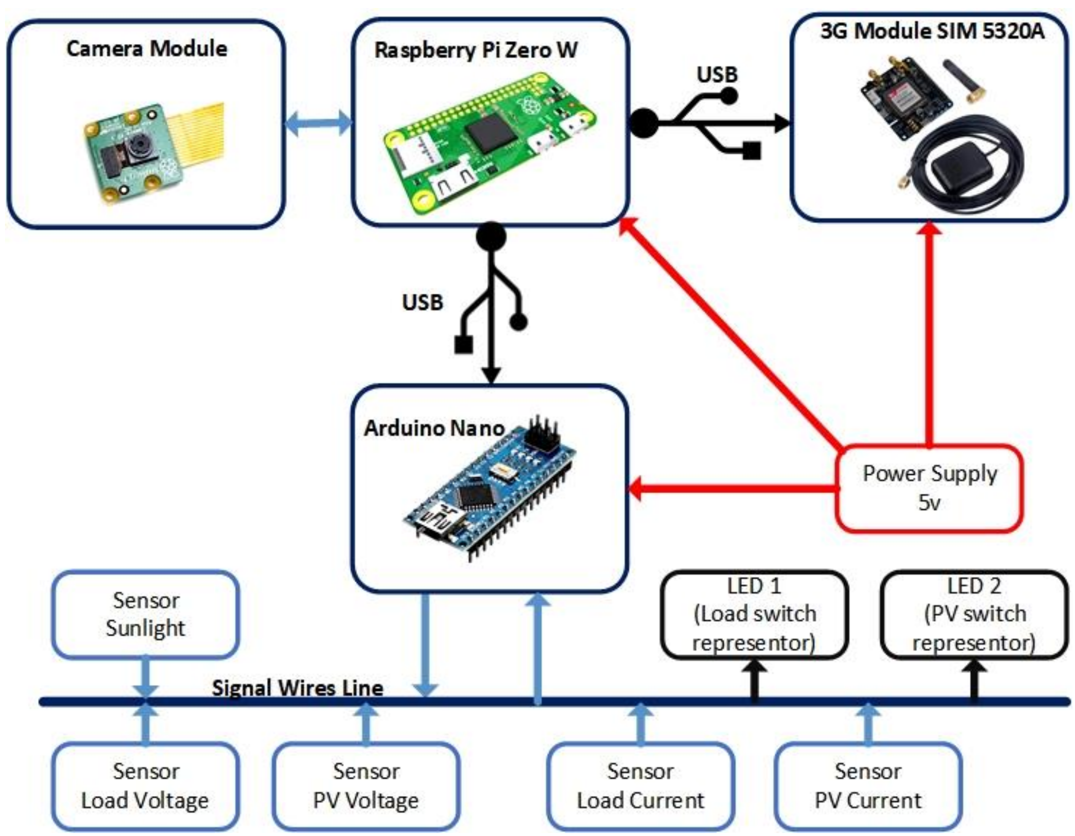

Figure 5.2: Block diagram of the server with various components

5.1.1 Voltage Sensor

In this research, a voltage divider using two resistors was designed to measure the voltages of the PV module and the load. The advantages of this type of sensor are its simplicity and low-cost. It can read an input voltage 0-25 votls and outputs a voltage between 0-5 volts which can be read by Arduino Nano's analog pins. Figure 5.3 shows the voltage devider sensor and its principle is shown in .

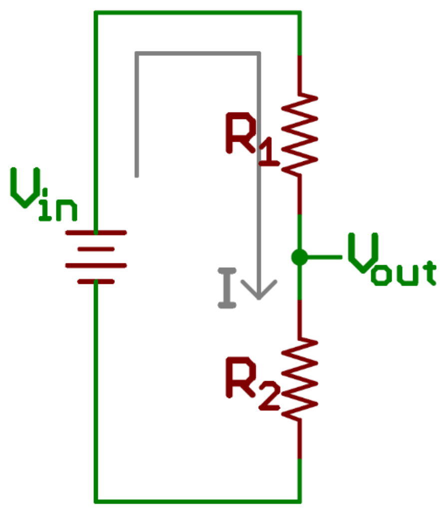

Figure 5.3: Voltage devider circuit

$$Vout = Vin * \frac{R1}{R1 + R2} \tag{4}$$

5.1.2 ACS 723 Hall-Effect Current Sensor

The ACS723 sensor is a high resolution sensor that uses a Hall-Effect IC to produce a voltage relative to the flow of current between the IP+ and IP- pins. Using this type of current sensor provides an advantage for the Arduino Nano microcontroller to electrically be isolated from the load side; it means that the output of the sensor operates at a low-voltage which is safe for the Arduino and the input of the sensor can operate at higher DC or AC voltages. Figure 5.4 shows an image of a hall-effect sensor.

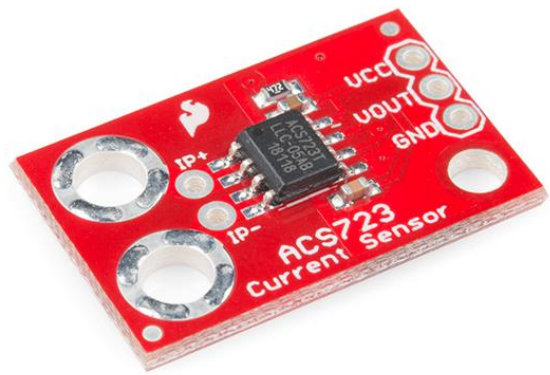

Figure 5.4 : ACS 723 Hall-Effect Sensor

5.1.3 Sunlight Sensor

A light sensor is a simple component that is designed to produce an analog or digital value according to the light intensity. In this research, a resistive light sensor is used in which the resistance across its terminals also change as the intensity of light changes. A simple circuit was designed using a light sensor and a resistor that allows Arduino to read a voltage relative ot the sunlight from its analog pins. Figure 5.5 shows an image of a sunlight.

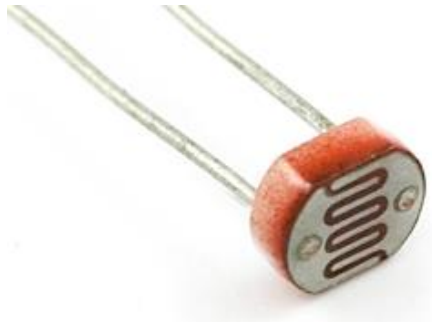

Figure 5.5: Light sensor

5.1.4 Wireless Connectivity

A wireless connection is a tremendous advantage for controlling systems in the era of modern technologies. In this regard, firstly, we took advantage of the raspberry pi's onboard WiFi module to connect it to the home router. In [43], there are complete instructions to implement a method called "headless" and operate the raspberry pi without any need to plug in a monitor, mouse, or keyboard, which, in turn, made the system more cost-efficient. Secondly, we set up a cellular connection using instructions in [44] and [45] to connect the server to a cellular 3G network. The cellular connection provides the server with the advantages of a cellular network, such as its availability.

5.1.5 Web-based Dashboard

In our system, we used Node-RED in programing the raspberry pi to create a server. Node-RED is a programming environment using various types of nodes (i.e., serial port nodes) and mouse-driven wiring nodes. Arduino is controlled through Node-RED through a very user-friendly editor based on the internet browser. We used the Node-red-dashboard node to create a graphical user interface where the server operator can execute the system for monitoring and controlling purposes.

Our system's final front end is a web-based graphical user interface, so-called dashboard, is shown in Figure 5.6 and Figure 5.7. There are two tabs in the dashboard: Main tab and Environment tab; the main tab, shown in Figure 5.6, contains historical charts for presenting electrical data such as voltage and current, gauges for showing instant electrical measurements of voltage and current, and switches to control two LEDs which represent the power switches in the system. The environment tab, shown in Figure 5.7, includes a jpg picture box with a button to take a photo that allows the user to monitor the field and sunlight data remotely. Using this dashboard, a user has complete remote control over the system from anywhere globally through 3G internet. The designed dashboard is developable, which the user can interact to monitor and control the solar water pump system in the garden. [46], [47]

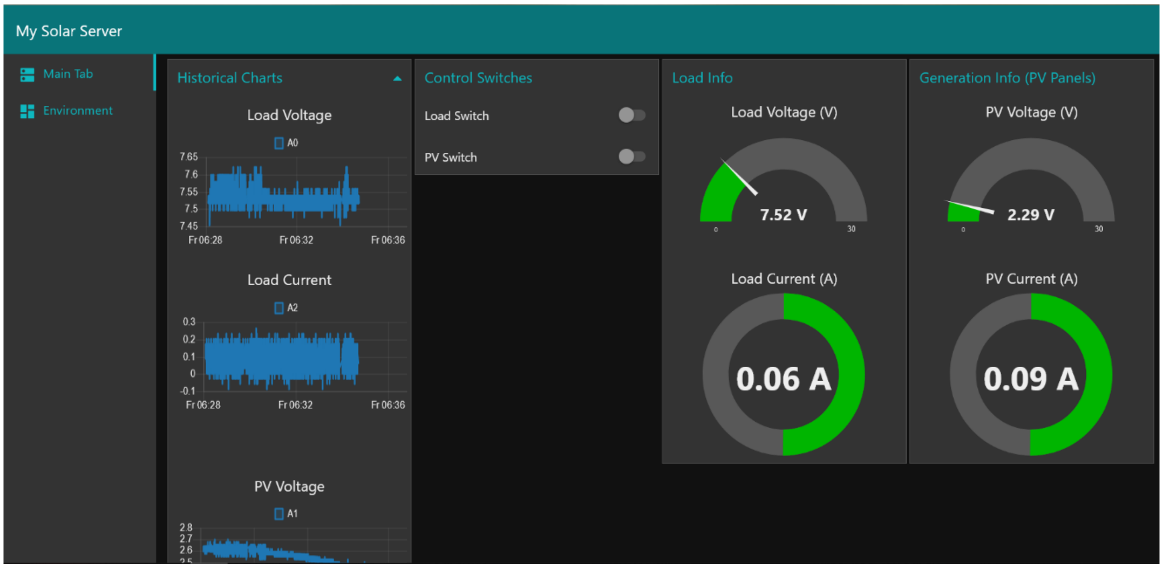

Figure 5.6: Dashboard Main Tab

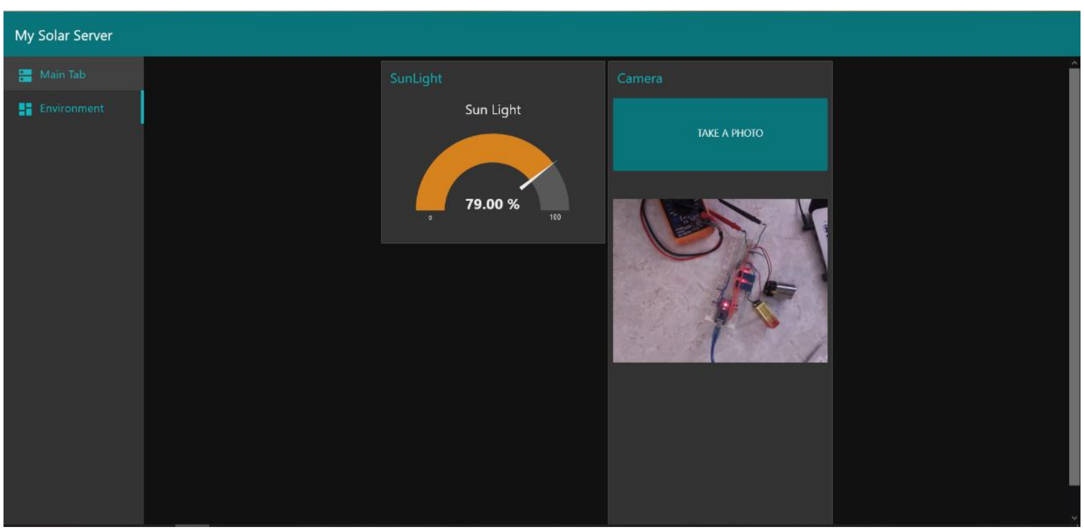

Figure 5.7: Dashboard Environment Tab

5.1.6 Communication with Arduino nano and electrical setup

Arduino nano is a small microcontroller board based on ATmega328 and has a meager power consumption. Using Arduino nano allows the server to sense and control various signals, such as analog signals for voltage measurement. There are many ways to communicate with an Arduino using Node-RED, such as Serial, Firmata, and Johnny-Five. We chose Firmata because it provides simplicity to the server and allows the computer to have direct access to the Arduino input and output pins.

In this setup, we designed a circuit to control two LEDs representing load and PV power switches and sensors to measure load and PV voltages, load and PV currents, and sunlight.

5.1.7 Exposing the server to the WEB and security

Since the user needs to access the server remotely, it needs to be published on a WEB server. The NGINX web server application was used on the raspberry pi to create a web server and publish the dashboard on that server. However, publishing a local server on the world wide web where a tremendous number of threats exist can put a very high risk on the server designed to monitor and control the solar water pumping system. Therefore, we set up an HTTP authentication with NGINX to solve security concerns; hence, the user needs to enter the username and the password of the server whenever connecting to the server IP address. The server is securely accessible through worldwide WEB, and server IP is also known to the user. [48]

5.1.8 Experimental Setup

The experimental setup of the SCADA server is shown in Figure 5.8.

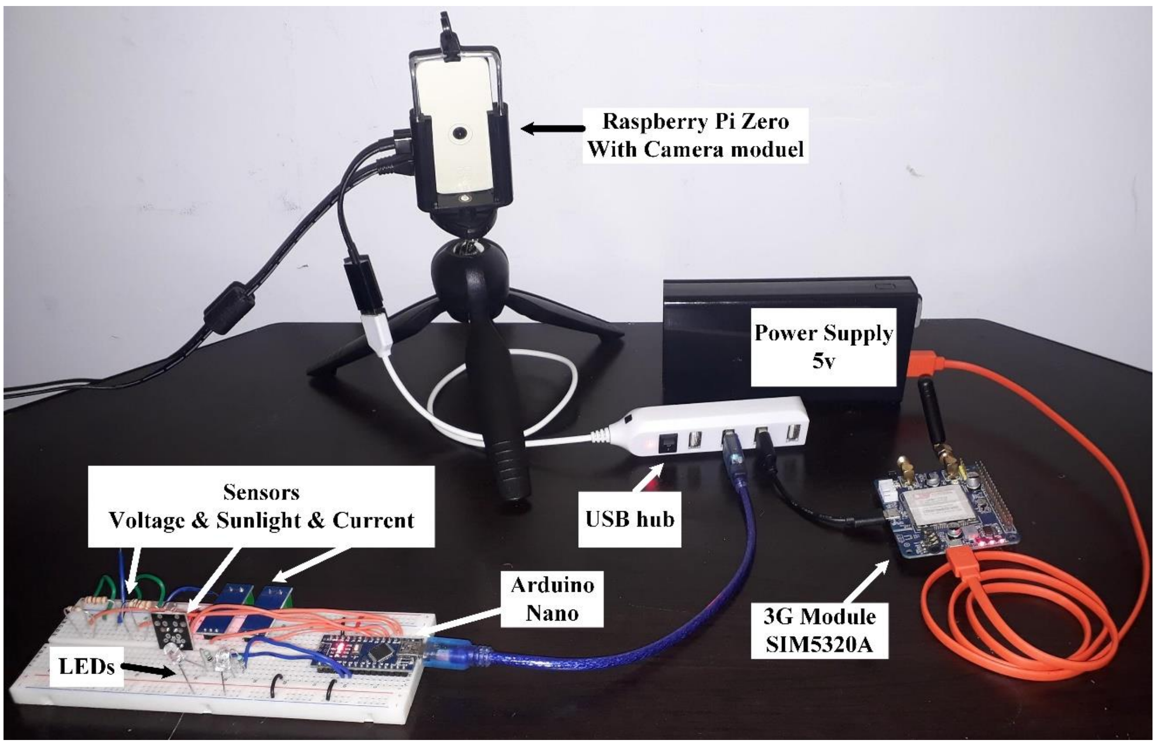

Figure 5.8: Experimental Setup of the SCADA server

5.2 Cost Analysis

The designed system is very cheap to install and use. The cost of the system includes a low power raspberry pi zero w (CDN$ 37.60), an Arduino nano (CDN$ 4.80), and a camera (CDN$ 13.99), and a 3G internet module SIM 5320A (CDN$ 105.99). We should note that the raspberry pi zero W has an onboard WiFi module that connects to an internet router when available. In this case, a 3G module is not required, and its price is waived.

In addition, the cost of high-speed internet service is very negligible; for instance, the cost of a one-year plan with 48 GB internet is about CAD$ 6.5 from a carrier named Irancell in Iran. This advantage allows our system to be very profitable in the long run. The total cost of the system is between CAD$ 56.39 to CAD$ 162.38, depending on which internet type we choose to use.

There are many IoT hubs in the market that share similarities with our proposed system. As an instance, Microsoft Azure IoT Hub is a product that provides a platform to connect, monitor, and control IoT devices. While the components required to implement an IoT SCADA application with Azure is almost at the same cost, it is required to pay an expensive monthly fee costing a minimum of 12.80 $CAD per each IoT Hub unit to implement the SCADA with it. It is worth mentioning that the number of messages communicated through IoT Hub in each plan is highly limited. This example shows the advantage of our designed system over other systems. Hence, the system is cost-effective compared to available IoT hubs such as Microsoft Azure in which the server is based on an internet cloud and is required to purchase their expensive plans. [49]

5.3 CONCLUSION

In this paper, the design of a cost-effective SCADA system for a solar water pumping system was presented. It consisted of a raspberry pi zero, Arduino nano, camera module, 3G module, and sensors for voltage, current, sunlight, and two LEDs. This server provides the system with a secure and complete monitoring and controlling GUI hub where the user can connect from anywhere through the internet and monitor and control a remote solar water pumping system. It is worth mentioning that the proposed system is implementable in any solar pumping system in the world where there is connectivity to the internet available. The only difference will be the cost of an internet plan from internet service providers.

Chapter 6 Conclusion & Future Work

6.1 Conclusion

The ongoing crises in Iran has brought the attention to execute this research and thesis; the main source of electrical energy generation is from fossil fuels and environmental water crisis. Therefore, it is vitally important to study researches that can help resolve these issues such as developing applications of renewable energy systems and enhancing the use of irrigation systems with high efficiency such as drip irrigation. In this thesis, a complete design and analysis of solar water pumping for drip irrigation of a 14.7 hectare grape garden is studied.

The study focuses on water requirement analysis of the fruit garden, electrical load sizing, design of the submersible water pumping systems, comparison of using storage systems (battery storage system and water tank), dynamic modelling and control in MATLAB/Simulink, design of an IoT-based SCADA system for monitoring and control of the field, and cost analysis of the systems. Based on the research, following items can be considered as main conclusions:

Solar water pumping technology is a reliable and economical technology. It provides an advantage to design irrigation systems with higher efficiency such as drip irrigation for remote places where the electricity grid is not accessible.

Using scientific tools such as FAO CropWat for water requirement analysis can result in proper irrigation scheduling and higher crop yield and consequently gives a precise load analysis for the research.

The cost analysis of using two types of storage systems, battery storage and water tank, shows that the battery storage system is a more economical solution. Although there are concerns around the lifecycle of the lead-acid battery storage system which can put doubts on the advantage of this type of storage system, since it is operated for a period of higher irrigation requirement (a short period of time in a year), it can operate for several years.

The dynamic modelling and simulation in MATLAB/Simulink shows that the battery storage based system operates completely fine and supports the load in different solar irradiance conditions.

The design of low-cost IoT-based SCADA is vital for the solar water pumping system because it provides an advantage to remotely monitor and control the solar water pumping system from any where in the world.

Research contributions:

- Water need determination and analysis
- Solar water pumping system design without battery storage system
- Solar water pumping design with battery storage system

- Modelling and simulation in MATLAB/Simulink
- IoT-based SCADA system design for a solar water pumping system

6.2 Future Work

Noting that the executed projects throughout this thesis were successful, there is still a huge need for more researches in this area. Followings are items to be considered for future work:

- The study and comparison of solar water pumping system for different locations in Iran need to be studied.
- It is suggested to study the impact of using solar water pumping in reducing the carbon emissons over a set period of time.
- It is suggested to study using solar water pumping in a vast number in a specific area. For example, in a city like Urmia, West Azerbayjan, the difference it can make to convert all types of irrigation systems into solar water pumping.
- The study and comparison of using solar water pumping for other types of fruits/crops needs to be done which will advance the solar water pumping technology. The common fruits/crops in Urmia West Azerbayjan are apples, cherries, apricot, grapes, wheat, cucurbits

- The study and comparison of solar water pumping for different types of irrigation systems can be studied such as flood irrigation, sprinkler irrigation, and micro-irrigation.
- The study and comparison of solar water pumping with different types of pumping systems need to be studied such as surface and sentrifusual submersible pumps.
- The study and comparison of regular pumping systems and solar water pumping need to be studied.
- The study and comparison of using different types of PV panels need to be done.
- The study and comparison of different types of battery storage systems need to be done.
- It is suggested to develop a simplified mathematical model of the system in Simulink. Therefore, the system can be simulated for a year or several years to observe its various components' responses. The designed dynamic model in this thesis takes a lot of time to only simulate the system for a short period because of the type of the Simulink blocks used in it.
- A dynamic model for solar water pumping systems with water tank storage can be developed. Therefore, two types of system structures can be compared with each other.

- Different types of IoT based SCADA systems can be developed to monitor various components conditions.

6.3 A list of publicaitons:

[1] M. Zamanlou, M. T. Iqbal, "Design and Analysis of Solar Water Pumping with Storage for Irrigation in Iran," 2020 IEEE 17th International Conference on Smart Communities: Improving Quality of Life Using ICT, IoT and AI (HONET), Virtual Conference, Charlotte, NC, USA

[2] C. A. Osaretin, M. Zamanlou, M. T. Iqbal, S. Butt, "Open Source IoT-Based SCADA System for Remote Oil Facilities Using Node-RED and Arduino Microcontrollers" 2020 IEEE Information Technology, Electronics and Mobile Communication Conference (IEMCON), Virtual Conference, Vancouver, BC, Canada

[3] M. Zamanlou and M. T. Iqbal, "Development of an Economical SCADA System for Solar Water Pumping in Iran," 2020 IEEE International IOT, Electronics and Mechatronics Conference (IEMTRONICS), Vancouver, BC, Canada, 2020, pp. 1-4, doi: 10.1109/IEMTRONICS51293.2020.9216408.

[4] A. M. Sharan, M. Zamanlou, "Energy Efficiency Enhancement of Electrical Vehicles," International Journal of Engineering and Applied Sciences (IJEAS), ISSN: 2394-3661, Volume-7, Issue-5, May 2020

[5] M. Zamanlou, M. T. Iqbal, “Design and analysis of a solar water pumping system for drip irrigation of a fruit garden in Iran,” The 28th Annual Newfoundland Electrical and Computer Engineering Conference (IEEE NECEC), 2019, St. John’s, NL, Canada

[6] A. M. Sharan, M. Zamanlou, “Accurate And Efficient Power Generation Of Photovotaic Systems Using Wireless Technology,” International Journal of Engineering and Applied Sciences (IJEAS), Volume-6, Issue-4, pp 2394-3661 April 2019

[7] A. M. Sharan, M. Zamanlou, Md. H. Rahman, Md. A. Al-Mehdi, “Centralized Power Generation of Solar Parks using Wireless Controlling,” 2019 International Journal of Current Engineering and Technology, Vol.9, No.3 (May/June 2019), pp 405-411

Invited Talk:

[1] Mohammad Zamanlou, “Design & Analysis of a Solar Water Pumping System for Micro Irrigation of a Fruit Garden,” IEEE NL Young Professionals Chapter Invited Technical Talk, December 2019

Bibliography

[1] S. S. Chandel, M. Nagaraju Naik, and R. Chandel, “Review of solar photovoltaic water pumping system technology for irrigation and community drinking water supplies,” *Renewable and Sustainable Energy Reviews*. 2015, doi: 10.1016/j.rser.2015.04.083.

[2] E. T. Maddalena, C. G. D. S. Moraes, G. Braganca, L. G. Junior, R. B. Godoy, and J. O. P. Pinto, “A Batery-Less Photovoltaic Water-Pumping System with Low Decoupling Capacitance,” in *IEEE Transactions on Industry Applications*, 2019, doi: 10.1109/TIA.2019.2900412.

[3] I. Yahyaoui, *Specifications of Photovoltaic Pumping Systems in Agriculture: Sizing, Fuzzy Energy Management and Economic Sensitivity Analysis*. 2016.

[4] “Iran - Countries & Regions - IEA.” [Online]. Available: https://www.iea.org/countries/iran. [Accessed: 24-Oct-2020].

[5] J. P. Evans and B. F. Zaitchik, “Modeling the large-scale water balance impact of different irrigation systems,” *Water Resour. Res.*, vol. 44, no. 8, Aug. 2008, doi: 10.1029/2007WR006671.

[6] “Water crisis in Iran - Wikipedia.” [Online]. Available: https://en.wikipedia.org/wiki/Water_crisis_in_Iran. [Accessed: 24-Oct-2020].

[7] “Water Crisis in Iran - Iran News Update.” [Online]. Available: https://irannewsupdate.com/news/society/water-crisis-in-iran/. [Accessed: 24-Oct-2020].

[8] A. Parvaresh Rizi, A. Ashrafzadeh, and A. Ramezani, “A financial comparative study of solar and regular irrigation pumps: Case studies in eastern and southern Iran,” *Renew. Energy*, vol. 138, pp. 1096–1103, 2019, doi: 10.1016/j.renene.2019.02.026.

[9] H. Ghasemi-Mobtaker, F. Mostashari-Rad, Z. Saber, K. wing Chau, and A. Nabavi-Pelesaraei, “Application of photovoltaic system to modify energy use, environmental damages and cumulative exergy demand of two irrigation systems-A case study: Barley production of Iran,” *Renew. Energy*, 2020, doi: 10.1016/j.renene.2020.07.047.

[10] L. O. Aghenta and M. T. Iqbal, “Low-cost, open source IoT-based SCADA system design using thinger.IO and ESP32 thing,” *Electron.*, 2019, doi: 10.3390/electronics8080822.

[11] C. Bepery, S. Baral, A. Khashkel, and F. Hossain, “Advanced Home Automation System Using Raspberry-Pi and Arduino,” *nternational J. Comput. Sci. Eng.*, vol. 8, no. 2, pp. 1–10, Feb. 2019.

[12] L. O. Aghenta and M. T. Iqbal, “Development of an IoT Based Open Source

SCADA System for PV System Monitoring," in *2019 IEEE Canadian Conference of Electrical and Computer Engineering, CCECE 2019*, 2019, doi: 10.1109/CCECE.2019.8861827.

[13] J. Lehr H. and J. Keeley, *Water Encyclopedia*. John Wiley & Sons, Inc., 2005.

[14] R. Mehta and V. Pandey, *Crop Water Requirement (Evapotranspiration And Estimation)*. 2018.

[15] "Crop water requirements," *FAO Irrig. Drain. Pap. No. 24, Food Agric. Organ. United Nations, Rome*, 1977.

[16] "CROPWAT - a computer program for irrigation planning and management," *FAO Irrig. Drain. Pap. No. 46, Food Agric. Organ. United Nations, Rome*, 1992.

[17] "CLIMWAT for CROPWAT," *FAO Irrig. Drain. Pap. No. 49, Food Agric. Organ. United Nations, Rome*, 1993.

[18] "Crop evapotranspiration - Guidelines for computing crop water requirements," *FAO Irrig. Drain. Pap. No. 56, Food Agric. Organ. United Nations, Rome*, 1998.

[19] "CONNECTED - LORENTZ." [Online]. Available: https://www.lorentz.de/products-and-technology/products/connected/. [Accessed: 26-Oct-2020].

[20] "PSk2-25 C-SJ95-4 | Lorentz Pumps." [Online]. Available:

https://lorentzpumps.co.za/product/psk2-25-c-sj95-4/. [Accessed: 26-Oct-2020].

[21] "PSk2-15 C-SJ42-6 | Lorentz Pumps." [Online]. Available: https://lorentzpumps.co.za/product/psk2-15-c-sj42-6/. [Accessed: 27-Oct-2020].

[22] "HOMER Pro - Microgrid Software for Designing Optimized Hybrid Microgrids." [Online]. Available: https://www.homerenergy.com/products/pro/index.html. [Accessed: 27-Oct-2020].

[23] "KianBattery." [Online]. Available: https://www.kianbattery.com. [Accessed: 27-Oct-2020].

[24] "Manasazan Shop." [Online]. Available: https://manasazan.ir/. [Accessed: 27-Oct-2020].

[25] "Engineer Plus | Ready Mix Concrete." [Online]. Available: https://engineerplus.ir/price/ready-mixed-concrete. [Accessed: 27-Oct-2020].

[26] "Introduction to DC-DC Converters." [Online]. Available: https://www.digikey.ca/en/maker/blogs/introduction-to-dc-dc-converters. [Accessed: 18-Nov-2020].

[27] "Design of switch power supplies." [Online]. Available: http://schmidt-walter-schaltnetzteile.de/smps_e/smps_e.html#Abw. [Accessed: 18-Nov-2020].

[28] "Buck converter - Wikipedia." [Online]. Available:

https://en.wikipedia.org/wiki/Buck_converter. [Accessed: 18-Nov-2020].

[29] "Buck Converter." [Online]. Available: http://schmidt-walter-schaltnetzteile.de/smps_e/abw_smps_e.

[30] "Boost converter - Wikipedia." [Online]. Available: https://en.wikipedia.org/wiki/Boost_converter. [Accessed: 18-Nov-2020].

[31] "Help for Boost Converter." [Online]. Available: http://schmidt-walter-schaltnetzteile.de/smps_e/aww_hilfe_e.html. [Accessed: 18-Nov-2020].

[32] "Pros and Cons of 60-cell & 72-cell Solar Modules | Coulee Limited." [Online]. Available: https://couleenergy.com/pros-and-cons-of-60-cell-72-cell-solar-modules/. [Accessed: 18-Nov-2020].

[33] "60 Cell vs. 72 Cell Solar Panels: Which is Right For You? | EnergySage." [Online]. Available: https://news.energysage.com/60-vs-72-cell-solar-panels-which-is-right/. [Accessed: 18-Nov-2020].

[34] "Boost Converter." [Online]. Available: http://schmidt-walter-schaltnetzteile.de/smps_e/aww_smps_e.html.

[35] N. Mendis, K. M. Muttaqi, S. Sayeef, and S. Perera, "A control approach for voltage and frequency regulation of a Wind-Diesel-battery based hybrid remote area power supply system," in *IECON 2010 - 36th Annual Conference on IEEE*

Industrial Electronics Society, 2010, pp. 3054–3060, doi: 10.1109/IECON.2010.5674969.

[36] N. H. Samrat, N. Bin Ahmad, I. A. Choudhury, and Z. Bin Taha, “Modeling, Control, and Simulation of Battery Storage Photovoltaic-Wave Energy Hybrid Renewable Power Generation Systems for Island Electrification in Malaysia,” *Sci. World J.*, vol. 2014, p. 436376, 2014, doi: 10.1155/2014/436376.

[37] M. Reda and R. Chenni, “Control Strategy for DC Bus Voltage Regulation in Photovoltaic System with Battery Energy,” *Int. J. Eng. Tech. Res.*, vol. 04, pp. 315–322, Aug. 2015.

[38] N. Mendis, K. M. Muttaqi, S. Perera, and M. N. Uddin, “Remote Area Power Supply System: An Integrated Control Approach Based on Active Power Balance,” *IEEE Ind. Appl. Mag.*, vol. 21, no. 2, pp. 63–76, Mar. 2015, doi: 10.1109/MIAS.2014.2345817.

[39] J. Chauhan, P. Chauhan, T. Maniar, and A. Joshi, “Comparison of MPPT algorithms for DC-DC converters based photovoltaic systems,” in *2013 International Conference on Energy Efficient Technologies for Sustainability, ICEETS 2013*, 2013, pp. 476–481, doi: 10.1109/ICEETS.2013.6533431.

[40] B. Subudhi and R. Pradhan, “A comparative study on maximum power point tracking techniques for photovoltaic power systems,” *IEEE Trans. Sustain. Energy*,

vol. 4, no. 1, pp. 89–98, 2013, doi: 10.1109/TSTE.2012.2202294.

[41] T. Selmi, M. Abdul-Niby, L. Devis, and A. Davis, "P&O MPPT implementation using MATLAB/Simulink," in *2014 9th International Conference on Ecological Vehicles and Renewable Energies, EVER 2014*, 2014, doi: 10.1109/EVER.2014.6844065.

[42] F. E. Tahiri, K. Chikh, M. Khafallah, and A. Saad, "Comparative study between two Maximum Power Point Tracking techniques for photovoltaic system," in *2016 International Conference on Electrical and Information Technologies (ICEIT)*, 2016, pp. 107–112, doi: 10.1109/EITech.2016.7519571.

[43] "How To Setup Raspberry Pi Zero W Headless WiFi - Tutorial Australia." [Online]. Available: https://core-electronics.com.au/tutorials/raspberry-pi-zerow-headless-wifi-setup.html. [Accessed: 06-Nov-2020].

[44] "How to setup a USB 3G Modem using usb_modeswitch and wvdial – Check BOT Tutorials." [Online]. Available: https://tchekbo.wordpress.com/2018/03/31/how-to-setup-a-usb-3g-modem-using-usb_modeswitch-and-wvdial/. [Accessed: 06-Nov-2020].

[45] "Raspberry Pi - Using a GPRS Modem for Network - YouTube." [Online]. Available: https://www.youtube.com/watch?v=T2NBpfgfPaI. [Accessed: 06-Nov-2020].

[46] “Node-RED.” [Online]. Available: https://nodered.org/. [Accessed: 06-Nov-2020].

[47] “node-red-dashboard (node) - Node-RED.” [Online]. Available: https://flows.nodered.org/node/node-red-dashboard. [Accessed: 06-Nov-2020].

[48] “How To Set Up HTTP Authentication With Nginx On Ubuntu 12.10 | DigitalOcean.” [Online]. Available: https://www.digitalocean.com/community/tutorials/how-to-set-up-http-authentication-with-nginx-on-ubuntu-12-10#prerequisites. [Accessed: 06-Nov-2020].

[49] “Pricing—IoT Hub | Microsoft Azure.” [Online]. Available: https://azure.microsoft.com/en-us/pricing/details/iot-hub/. [Accessed: 06-Nov-2020].

Appendix

Perturbation and Observation code implemented in Simulink.

Editor - Block: FinalProj/ Controller Unit/MPPT Controller using Perturbe & Observe technique

Controller Unit/MPPT Controllerusing Perturbe & Observe technique | Controller Unit/Battery Overcharge Protection.

```
function D  = MPPT(Param, Enabled, V, I)

% MPPT controller based on the Perturb & Observe algorithm.

% D output = Duty cycle of the boost converter (value between 0 and 1)
%
% Enabled input = 1 to enable the MPPT controller
% V input = PV array terminal voltage (V)
% I input = PV array current (A)
%
% Param input:
Dinit = Param(1);  %Initial value for D output
Dmax = Param(2);   %Maximum value for D
Dmin = Param(3);   %Minimum value for D
deltaD = Param(4); %Increment value used to increase/decrease the duty cycle D
% ( increasing D = decreasing Vref )
%

persistent Vold Pold Dold;

dataType = 'double';

if isempty(Vold)
    Vold=0;
    Pold=0;
    Dold=Dinit;
end
P= V*I;
dV= V - Vold;
dP= P - Pold;

```

```
if dP ~= 0 && Enabled ~=0
    if dP < 0
        if dV < 0
            D = Dold - deltaD;
        else
            D = Dold + deltaD;
        end
    else
        if dV < 0
            D = Dold + deltaD;
        else
            D = Dold - deltaD;
        end
    end
else D=Dold;
end

if D >= Dmax | D<= Dmin
    D=Dold;
end

Dold=D;
Vold=V;
Pold=P;
end
```

MATLAB code for load control

Controller Unit/Battery Over-Discharge & DC Link VoltageController.

```
function LC  = LCS(SOC, Vdc, Rstrct, Enabled)


% Restrictions input:
SOC_min = Rstrct(1);  %Minimum value for State of Charge of the battery
SOC_mrgn= Rstrct(2);  %Margine of SOC from Minimum value to returning on the switch
Vdc_max = Rstrct(3);   %Maximum value for Dc Link voltage
Vdc_min = Rstrct(4);   %Minimum value for DC link Voltage

LC=1;
if Enabled ~=0
    if  (Vdc > Vdc_min && Vdc< Vdc_max)
        if (SOC > (SOC_min + SOC_mrgn))
            LC=1;
        elseif (SOC < SOC_min)
            LC=0;
        end
    else
        LC=0;
    end
else
    LC=1;
end
end

```